Long-term evolution and revival structure of Rydberg wave packets for hydrogen and alkali-metal atoms

Robert Bluhm[1] and V. Alan Kostelecký[2]
[1]*Physics Department, Colby College, Waterville, Maine 04901*
[2]*Physics Department, Indiana University, Bloomington, Indiana 47405*
(Received 31 May 1994; revised manuscript received 20 December 1994)

This paper begins with an examination of the revival structure and long-term evolution of Rydberg wave packets for hydrogen. We show that after the initial cycle of collapse and fractional or full revival, which occurs on the time scale t_{rev}, a new sequence of revivals begins. We find that the structure of the new revivals is different from that of the fractional revivals. The new revivals are characterized by periodicities in the motion of the wave packet with periods that are fractions of the revival time scale t_{rev}. These long-term periodicities result in the autocorrelation function at times greater than t_{rev} having a self-similar resemblance to its structure for times less than t_{rev}. The new sequence of revivals culminates with the formation of a single wave packet that more closely resembles the initial wave packet than does the full revival at time t_{rev}, i.e., a superrevival forms. Explicit examples of the superrevival structure for both circular and radial wave packets are given. We then study wave packets in alkali-metal atoms, which are typically used in experiments. The behavior of these packets is affected by the presence of quantum defects that modify the hydrogenic revival time scales and periodicities. Their behavior can be treated analytically using supersymmetry-based quantum-defect theory. We illustrate our results for alkali-metal atoms with explicit examples of the revival structure for radial wave packets in rubidium.

PACS number(s): 32.80.Bx, 03.65.−w

I. INTRODUCTION

A localized electron wave packet is formed when a short-pulsed laser excites a coherent superposition of Rydberg states [1,2]. Wave packets of this type offer the opportunity to investigate the classical limit of the motion of electrons in Rydberg atoms. Initially, the motion of the wave packet follows the classical motion of a charged particle in a Coulomb field. The period of the motion is the classical period T_{cl} of a particle in a Keplerian orbit. However, this motion persists only for a few cycles, whereupon quantum interference effects cause the wave packet first to collapse and then to undergo a sequence of revivals [1–4]. The revivals are characterized by the recombination of the collapsed wave packet into a form close to the original shape, which again oscillates with period T_{cl}. The recombined wave packet is called a full revival and it appears at a time t_{rev}. For various times earlier than t_{rev}, the wave packet gathers into a series of subsidiary wave packets called fractional revivals. The motion of these fractional revivals is periodic, with a period equal to a rational fraction of the classical Keplerian period.

This cycle of collapse, fractional revivals, and full revival is characteristic of several distinct types of Rydberg wave packets. Among these are radial, circular, and elliptical packets. A radial wave packet is localized in the radial coordinate but is in a definite eigenstate of the angular momentum. A circular wave packet is a superposition of fully aligned eigenstates with maximal values of the angular-momentum quantum numbers. It is localized in both angular and radial coordinates and it follows a circular trajectory. Lastly, an elliptical wave packet is localized in all three dimensions and travels along a classical Keplerian orbit.

Recently, there has been much experimental interest in the study of these Rydberg wave packets. Radial wave packets can be formed by the excitation of the atom from the ground state by a short-pulsed laser. The time evolution of the wave packet may then be studied using a pump-probe method of detection involving either time-delayed photoionization [2] or phase modulation [5–7]. The periodic motion of the radial wave packet, with the period equal to the classical orbital period, has been observed [8,9], and full and fractional revivals have been seen experimentally [10–12]. Circular states have been produced as well, using either the adiabatic microwave transfer method [13] or crossed electric and magnetic fields [14]. These methods excite a range of states in a fixed n manifold, resulting in a wave packet that is stationary. A technique for the excitation of circular-orbital states to generate a circular wave packet has been proposed [15]. If an additional weak electric field is present, an elliptical wave packet of arbitrary eccentricity could be produced.

Several theoretical approaches have been used to study the properties of Rydberg wave packets. Some involve a description via different types of coherent states [16]. Radial wave packets have been studied both numerically [1] and perturbatively [2] and recently a description as a type of squeezed state has been obtained [17,18]. They exhibit oscillations in the uncertainty product characteristic of a squeezed state. These states undergo full and fractional revivals with localized subsidiary waves distributed along

the radial direction. In contrast, the coherent-state approaches dealing with circular and elliptical states [19–25] all involve superpositions of angular-momentum eigenstates and/or large angular-momentum quantum numbers. The simplest such state is a circular wave packet consisting of a superposition of aligned eigenstates weighted by a Gaussian function [25]. These have been studied numerically and exhibit both fractional and full revivals. The subsidiary waves that form in this case are at a fixed radius and are distributed in the azimuthal angle.

Most work on the evolution of Rydberg wave packets has focused on the structure of the fractional revivals, which occur at times less than $t_{\rm rev}$. In this paper, we examine the evolution and revival structure of Rydberg wave packets for times *beyond* the revival time. We find that after a few revival cycles the wave packet ceases to reform at multiples of the revival time. Instead, a new sequence of collapses and revivals begins that is different from that of the usual fractional revivals. This sequence culminates with the formation of a wave packet that better resembles the original packet than does the full revival at time $t_{\rm rev}$. We refer to packets of this new type as superrevivals.

The appearance of the superrevivals is controlled by a new time scale $t_{\rm sr}$. We find that at certain times $t_{\rm frac}$ *before* $t_{\rm sr}$, the wave function can be written as a sum of macroscopically distinct subsidiary waves. Their motion is periodic with period $T_{\rm frac}$ given in terms of $t_{\rm rev}$ and $T_{\rm cl}$. This periodicity is on a much longer time scale than that of the usual fractional revivals. For times greater than $t_{\rm rev}$, it produces in the autocorrelation function a self-similar resemblance to its appearance at times less than $t_{\rm rev}$.

In addition to presenting the above qualitative features of the new revival structure, this paper discusses a quantitative theory providing detailed expressions for the various time scales and periodicities that appear. The features of the theory are illustrated with explicit examples for both circular and radial wave packets. In these examples, we first consider wave packets having large values of the principal quantum number n, since these display detailed features of the superrevivals most strikingly. We then consider wave packets with smaller values of n for which the time scales for the superrevival structure fall within a range currently accessible in experiment.

The above discussion applies to wave packets in hydrogen. In the latter part of this paper, we extend our analysis to obtain an analytical description for the case of Rydberg wave packets in alkali-metal atoms, typically examined in experiments. Examples are given to illustrate the resulting modifications of the behavior. The issue of distinguishing effects on the revival times and periodicities caused by the quantum defects from those caused by a detuning of the laser has been considered in Ref. [26]. In fact, not only are the effects different, but also the quantum-defect modifications to long-term revival times cannot be obtained by a direct scaling of the hydrogenic results.

The structure of this paper is as follows. Section II presents the generic form we use for circular and radial wave packets and introduces the distinct time scales $T_{\rm cl}$, $t_{\rm rev}$, and $t_{\rm sr}$ determining wave-packet behavior over the time period of interest. In Sec. III we examine the long-term behavior of Rydberg wave packets for hydrogen. We show that at certain times $t_{\rm frac}$ the wave function is well approximated as a sum over subsidiary waves with specified coefficients and we present constraints on the allowed values of $t_{\rm frac}$. We also demonstrate that at these times the motion of the subsidiary wave packets is periodic with a period $T_{\rm frac}$ dependent on $t_{\rm rev}$ and $T_{\rm cl}$. The periodicity of the autocorrelation function is analyzed. Section IV provides illustrative examples of circular and radial wave packets in hydrogen both for large values of n and for smaller values that are experimentally viable.

In Sec. V we extend our results to the case of wave packets in alkali-metal atoms, establishing the modifications in the revival time scales and periodicities that result from the inclusion of quantum defects. Explicit examples for the case of rubidium are provided in Sec. VI. Section VII discusses the results and considers some of the issues involved in experimental verification of our theory. Throughout the paper, technical details of the various proofs are relegated to the Appendixes.

II. TIME SCALES FOR WAVE-PACKET EVOLUTION

This section establishes some notation and conventions and provides a brief review of the evolution of Rydberg wave packets in hydrogen for times up to the revival time $t_{\rm rev}$. In Sec. II A we present the wave function we use throughout the paper for the analysis. It is a generic form that permits simultaneous treatment of circular and radial wave packets. In Sec. II B we expand the component eigenenergies in a Taylor series about the wave-packet energy. This leads to the definition of distinct time scales governing the evolution of the wave function. Some background on the behavior of hydrogenic wave packets for times up to $t_{\rm rev}$ is given in Sec. II C, along with an example.

A. Circular and radial wave packets

The time-dependent wave function for a hydrogenic wave packet may be expanded in terms of energy eigenstates as

$$\Psi(\vec{r},t)=\sum_{n,l,m} c_{nlm}\psi_{nlm}(\vec{r})\exp[-iE_n t]\ . \tag{1}$$

Here $E_n=-1/2n^2$ is the energy in atomic units and $\psi_{nlm}(\vec{r})$ is a hydrogen eigenstate of energy and angular momentum. The weighting coefficients $c_{nlm}=\langle\psi_{nlm}(\vec{r})|\Psi(\vec{r},0)\rangle$ depend on the initial wave function.

Two types of wave packets used in experiments are considered in this paper. The first type is the *circular* wave packets, which consist of a sum of fully aligned eigenstates, i.e., ones with $l=m=n-1$. In this case, the sum in Eq. (1) reduces to a sum over n alone, and the

weighting coefficients c_n are independent of l and m. The second type is the *radial* wave packets, which consist of a sum of eigenstates with fixed angular-momentum quantum number. For example, all the eigenstates may be p states. Once again, the sum in Eq. (1) depends only on n, and we may drop the l and m subscripts on c_n.

Adopting the generic notation that $\varphi_n(\vec{r})$ represents the eigenstates appropriate to a given type of wave packet, we may then rewrite Eq. (1) as

$$\Psi(\vec{r},t)=\sum_{n=1}^{\infty} c_n\varphi_n(\vec{r})\exp[-iE_n t] \ . \tag{2}$$

For the circular wave packets $\varphi_n(\vec{r})=\psi_{n,n-1,n-1}(\vec{r})$, while for the radial wave packets $\varphi_n(\vec{r})=\psi_{n,1,0}(\vec{r})$.

Both types of wave packet are excited by a short laser pulse. Since the laser can be tuned to excite coherently a superposition of states centered on a mean value of the principal quantum number $\bar{n}$, in what follows we assume that the distribution is strongly centered around a value $\bar{n}$. We may therefore approximate the square of the weighting coefficients as a Gaussian function

$$|c_n|^2=\frac{1}{\sqrt{2\pi\sigma^2}}e^{-(n-\bar{n})^2/2\sigma^2} \ . \tag{3}$$

In the derivations that follow, we take $\bar{n}$ to be an integer. The results can readily be extended to incorporate noninteger $\bar{n}$. The effects of noninteger $\bar{n}$ and the consequences of laser detuning are examined in Ref. [26].

B. Time scales

If we expand the energy in a Taylor series around the centrally excited value $\bar{n}$, we obtain

$$E_n\simeq E_{\bar{n}}+E'_{\bar{n}}(n-\bar{n})+\tfrac{1}{2}E''_{\bar{n}}(n-\bar{n})^2 +\tfrac{1}{6}E'''_{\bar{n}}(n-\bar{n})^3+\cdots \ , \tag{4}$$

where each prime on $E_{\bar{n}}$ denotes a derivative. The terms with derivatives define distinct time scales that depend on $\bar{n}$. The first time scale,

$$T_{\rm cl}=\frac{2\pi}{E'_{\bar{n}}}=2\pi\bar{n}^3 \ , \tag{5}$$

is the classical Keplerian period. It controls the initial behavior of the packet. The second time scale,

$$t_{\rm rev}=\frac{-2\pi}{\frac{1}{2}E''_{\bar{n}}}=\frac{2\bar{n}}{3}T_{\rm cl} \ , \tag{6}$$

is the revival time. It governs the appearance of the usual fractional and full revivals.

The subject of this paper is the behavior of the packet on time scales greater than $t_{\rm rev}$. This behavior is dominantly controlled by a third time scale,

$$t_{\rm sr}=\frac{2\pi}{\frac{1}{6}E'''_{\bar{n}}}=\frac{3\bar{n}}{4}t_{\rm rev} \ . \tag{7}$$

The scale $t_{\rm sr}\gg t_{\rm rev}$ is a larger time scale we refer to as the superrevival time. Note that although $t_{\rm sr}$ is large (typically about two orders of magnitude greater than $t_{\rm rev}$) for the range of $\bar{n}$ of interest, it is still much smaller than the lifetime of the excited Rydberg atom. It is also smaller than the typical time scales for which microwave blackbody radiation causes transitions [27]. It is therefore experimentally and theoretically reasonable to examine the behavior of the packet on this time scale.

Keeping terms through third order and defining the integer index $k=n-\bar{n}$, we may rewrite Eq. (2) as

$$\Psi(\vec{r},t)=\sum_{k=-\infty}^{\infty} c_k\varphi_k(\vec{r}) \times\exp\left[-2\pi i\left[\frac{kt}{T_{\rm cl}}-\frac{k^2t}{t_{\rm rev}}+\frac{k^3t}{t_{\rm sr}}\right]\right] . \tag{8}$$

We assume that $\bar{n}$ is large so that the lower limit in the sum may be approximated by $-\infty$. In this notation c_k and $\varphi_k(\vec{r})$ represent $c_{n=k+\bar{n}}$ and $\varphi_{n=k+\bar{n}}(\vec{r})$, respectively.

C. Review of behavior within the revival time scale

This subsection briefly summarizes the known behavior of the packet within the revival time scale and provides an example useful for comparison in our later analysis.

The quantum evolution of the wave function (2) up to times of order $t_{\rm rev}$ is governed by the first two terms in the exponential function in Eq. (8). If only the term linear in k were present, the wave packet would evolve like any localized packet for the harmonic oscillator, following the classical motion and oscillating indefinitely with period $T_{\rm cl}$.

The higher-order terms modify this behavior. The term quadratic in k governs the collapse and revival of the packet for times within $t_{\rm rev}/n$. An analysis of the role of this term is given in Ref. [3], where it is shown that at the times $t\approx mt_{\rm rev}/n$, where m and n are relatively prime integers, the wave packet may be rewritten approximately as an equally weighted sum of subsidiary wave packets. These are the usual fractional revivals.

The behavior of the fractional revivals may be studied by examining the absolute square of the autocorrelation function [4],

$$|A(t)|^2=\left|\sum_n |c_n|^2 e^{-iE_n t}\right|^2 \ . \tag{9}$$

Since the wave function $\varphi_n(\vec{r})$ has been integrated over, we find the same autocorrelation function and hence the same revival structure for both circular and radial wave packets. At the fractional-revival times $t\approx mt_{\rm rev}/n$, the autocorrelation function is periodic with fractional periods $T_{\rm cl}/r$, where r denotes the number of subsidiary wave packets.

An example useful for comparison with our analyses below is a wave packet in hydrogen centered about $\bar{n}=319$ with $\sigma=2.5$. Figure 1 shows the square of the autocorrelation function for times up to and just beyond $t_{\rm rev}\simeq 1.05$ μsec. Fractional revivals are prominent at $t\approx\frac{1}{8}t_{\rm rev}\simeq 0.13$ μsec, $t\approx\frac{1}{6}t_{\rm rev}\simeq 0.18$ μsec, $t\approx\frac{1}{4}t_{\rm rev}\simeq 0.26$

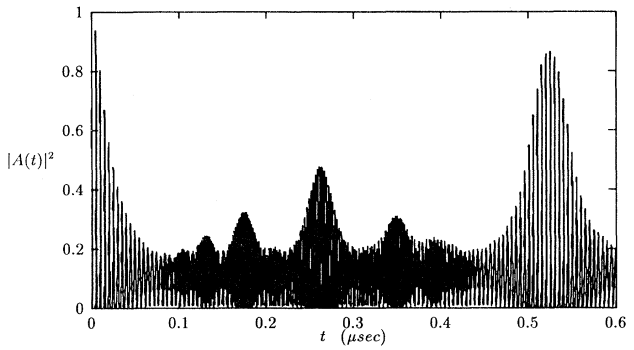

(a)

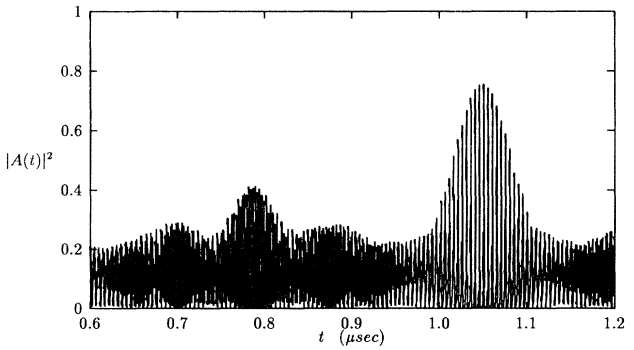

(b)

FIG. 1. The absolute square of the autocorrelation function for a hydrogenic Rydberg wave packet with $\bar{n}=319$ and $\sigma=2.5$ is plotted as a function of time in microseconds. The plots span times of order of the revival time $t_{\rm rev}\simeq 1.05$ μsec. (a) $t=0$–0.6 μsec and (b) $t=0.6$–1.2 μsec.

μsec, $t\approx\frac{1}{2}t_{\rm rev}\simeq 0.53$ μsec, and at multiples of these values. The periodicity of the autocorrelation function at the one-half and full revivals is $T_{\rm cl}\simeq 4.9$ nsec. This can be seen in the figure. The periodicities at the earlier fractional revivals, for $t\approx\frac{1}{8}t_{\rm rev},\frac{1}{6}t_{\rm rev},\frac{1}{4}t_{\rm rev}$, respectively, are $\frac{1}{4}T_{\rm cl},\frac{1}{3}T_{\rm cl},\frac{1}{2}T_{\rm cl}$. As can be observed in the figure, the peaks in the autocorrelation function are not as pronounced for times approaching $t_{\rm rev}$ as they are for earlier times. This is because higher-order terms in the energy expansion (4) act to distort the revivals.

III. WAVE PACKETS IN HYDROGEN

In this section, we show that at certain times $t_{\rm frac}$ it is possible to expand the third-order wave function $\Psi(\vec{r},t)$ of Eq. (8) as a series of subsidiary wave functions. Following Ref. [3], the idea is to express $\Psi(\vec{r},t)$ as a sum of wave functions $\psi_{\rm cl}$ with matching periodicities and with a shape similar to that of the initial wave function $\Psi(\vec{r},0)$. The form of the coefficients in the expansion of $\Psi(\vec{r},t)$ is obtained and used to show that at times $t_{\rm frac}$ the expansion correctly reproduces the wave function. At particular values of $t_{\rm frac}$, superrevivals are shown to form that more closely resemble the initial wave packet than does the full revival. Lastly, we show that the wave function and the autocorrelation function are periodic with a given period $T_{\rm frac}$.

In what follows, we find it is useful to write the times $t_{\rm frac}$ at which the subsidiary wave packets form as a linear combination of rational fractions of $t_{\rm sr}$ and $t_{\rm rev}$. We therefore define

$$t_{\rm frac}=\frac{p}{q}t_{\rm sr}-\frac{m}{n}t_{\rm rev}\ , \tag{10}$$

where p and q are relatively prime integers, as are m and n. Constraints on the possible values of these integers are derived below. In particular, we find that m is nonzero whenever $\bar{n}$ cannot be evenly divided by 4. We therefore write $\bar{n}$ as

$$\bar{n}=4\eta+\lambda\ , \tag{11}$$

where η and λ are both integers, and $\lambda=0$, 1, 2, or 3.

The subsidiary wave functions we use in the expansion of the full wave function are defined in terms of a function $\psi_{\rm cl}$ depending only on the first-derivative term in the energy expansion,

$$\psi_{\rm cl}(\vec{r},t)=\sum_{k=-\infty}^{\infty}c_k\varphi_k(\vec{r})\exp\left[-2\pi i\frac{2\bar{n}}{3}\frac{kt}{t_{\rm rev}}\right]\ . \tag{12}$$

We write it in terms of $t_{\rm rev}$ instead of $T_{\rm cl}$ because the former is more useful when considering times greater than $t_{\rm rev}$.

The subscript on $\psi_{\rm cl}$ is a reminder that this wave function follows the classical motion at all times. Note also that at time zero, $\psi_{\rm cl}(\vec{r},0)=\Psi(\vec{r},0)$, i.e., $\psi_{\rm cl}(\vec{r},0)$ matches the initial wave function exactly. These features of the function $\psi_{\rm cl}(\vec{r},t)$ make it a suitable candidate for use in generating an expansion of the full wave function $\Psi(\vec{r},t)$ as a sum of macroscopically distinct subsidiary wave functions.

Appendix A shows that at the times $t_{\rm frac}$ the wave function $\Psi(\vec{r},t)$ can be written as a sum of subsidiary waves having the form of $\psi_{\rm cl}(\vec{r},t)$, but at times that are shifted by a fraction of the period $T_{\rm cl}$. The shifted functions have the form $\psi_{\rm cl}(\vec{r},t+(s\alpha/l)T_{\rm cl})$, where l and α are certain specified integers and $s=0,1,2,\ldots,l-1$. Since these functions form a set with the same periodicity as $\Psi(\vec{r},t)$ at the times $t_{\rm frac}$, we can use them as a basis for expanding $\Psi(\vec{r},t)$. Moreover, the shapes of the shifted $\psi_{\rm cl}$ resemble the initial wave function at different points in its cycle, after it has been time translated by a fraction of the classical period $T_{\rm cl}$. An expansion of this type provides a natural formalism within which to examine the occurrence of long-term revivals.

We therefore write an expansion in subsidiary wave functions at times $t\approx t_{\rm frac}$ in the form

$$\Psi(\vec{r},t)=\sum_{s=0}^{l-1}b_s\psi_{\rm cl}\left[\vec{r},t+\frac{s\alpha}{l}T_{\rm cl}\right]\ . \tag{13}$$

The coefficients b_s are complex valued and are given as

$$b_s = \frac{1}{l} \sum_{k'=0}^{l-1} \exp\left[2\pi i \frac{\alpha s}{l} k'\right] \exp[2\pi i \theta_{k'}] , \quad (14)$$

where θ_k is defined in Eq. (A3) of Appendix A.

Appendix A also derives the constraints on the integers p, q, m, and n in the definition (10) of $t_{\rm frac}$ and shows that $p=1$, q is a multiple of 3, and m/n obeys Eq. (A2). With these constraints, the expansion of $\Psi(\vec{r},t)$ in terms of subsidiary waves $\psi_{\rm cl}(\vec{r},t)$ holds at times $t_{\rm frac}$ given by Eq. (10). Since $t_{\rm sr} \gg t_{\rm rev}$, we conclude that interesting behavior of the wave packet can be expected near times that are simple fractions of $\frac{1}{3}t_{\rm sr}$. This somewhat counterintuitive result is strongly supported by the examples presented in Sec. IV.

Whereas the usual fractional revivals consist of r subsidiary packets weighted equally by factors of $1/r$ and hence have fractional period $T=T_{\rm cl}/r$, we find that the superrevivals have a different behavior. An interesting feature of the b_s coefficients (14) at the times $t_{\rm frac}$ is that they may have *different* moduli $|b_s|^2$ and hence distinct subsidiary wave packets may not all have the same weight. Explicit examples of this are given in Sec. IV. In certain cases, all the b_s coefficients except one vanish. The remaining one then has modulus one, corresponding to the formation of one wave packet. It turns out that at the times $t_{\rm frac}$, even if the subsidiary wave packets are unequally weighted, the wave packet and the autocorrelation function are periodic.

In what follows, it is useful to introduce terminology distinguishing the different types of superrevival that can appear. We refer to the set of subsidiary packets at the times $t_{\rm frac}$ as a *fractional* superrevival. However, occasionally only a single packet appears, resembling the initial wave packet more closely than the usual full revival does at the time $t_{\rm rev}$. This is because contributions are incorporated from higher-order corrections in the expansion of the time-dependent phase. We call a single wave packet of this type a *full* superrevival.

After the formation of a fractional superrevival consisting of several subsidiary wave packets, it often happens that the subsidiary packets quickly evolve into a configuration where one of them is much larger than the others. The dominant wave packet in this case can again resemble the initial wave packet more closely than does the full revival at time $t_{\rm rev}$. We refer to a configuration of this type, consisting of primarily one large wave packet, as a *partial* superrevival.

Appendix B proves that the wave packet $|\Psi(\vec{r},t)|^2$, as well as the absolute square of the autocorrelation function $A(t_{\rm frac}) = \langle \Psi(\vec{r},0) | \Psi(\vec{r},t_{\rm frac}) \rangle$, is periodic at times $t \approx t_{\rm frac}$. The period $T_{\rm frac}$ is given as

$$T_{\rm frac} = \frac{3}{q} t_{\rm rev} - \frac{u}{v} T_{\rm cl} , \quad (15)$$

where the integers u and v satisfy Eq. (B17). In addition, the value of p in $t_{\rm frac}$ must equal 1 for this periodic behavior to occur.

This periodicity is different from that of the usual fractional revivals, for which the periods are fractions of $T_{\rm cl}$. Instead, the periods of the fractional superrevivals are fractions of $t_{\rm rev}$ combined with small additional shifts that depend on $T_{\rm cl}$. The time scale is considerably greater for the fractional superrevivals than for the fractional revivals. In addition, this periodicity causes the autocorrelation function for times much greater than $t_{\rm rev}$ to have a self-similar resemblance to its form for times less than $t_{\rm rev}$. We will illustrate this behavior explicitly in the next section.

IV. EXAMPLES FOR HYDROGEN

This section presents several examples illustrating in detail the various aspects of the long-term evolution of Rydberg wave packets in hydrogen. Results numerically generated from analytical expressions are compared with the theoretical predictions given above.

In these examples, we assume that the laser is tuned to excite coherently a distribution strongly centered at either $\bar{n}=319$ or 36. The former is large and ensures that interesting features of the superrevival structure are noticeable. Since 319 is not divisible by 4, the quantity λ in Eq. (11) is nonzero, which in turn makes the ratio m/n nonzero in the definition of $t_{\rm frac}$. The full analysis of Sec. III is therefore required. An example with $\bar{n}=320$, which is divisible by 4, can be found in Ref. [28].

The other choice, $\bar{n}=36$, is motivated by experimental considerations. For this case, the associated time delay in a pump-probe experiment falls within a range that is currently accessible. Our analysis shows that the corresponding full supperrevival occurs after approximately 776 psec, which is within the range of time delays considered in Refs. [10,11].

Section IV A examines the autocorrelation functions for the example with $\bar{n}=319$. Since the autocorrelation functions for corresponding circular and radial wave packets are identical, this provides a relatively broad perspective on the long-term behavior. In Sec. IV B, we examine detailed features of circular wave packets with $\bar{n}=319$ at the times $t_{\rm frac}$. Hydrogenic radial wave packets with the experimentally accessible value $\bar{n}=36$ are considered in Sec. IV C.

A. Autocorrelation functions

This subsection discusses the autocorrelation functions for our two choices of $\bar{n}$. The absolute squares of the autocorrelation functions are computed directly using the analytical expression in Eq. (9) and the definition of the c_n coefficients given in Eq. (3). These results are then compared with the preceding theoretical analysis. In what follows, we restrict ourselves to times of order $\frac{1}{6}t_{\rm sr}$, corresponding to a minimum value of q equal to 6. An accurate treatment on longer time scales requires fourth- and higher-order terms in the Taylor-series expansion of the energy.

The autocorrelation function is primarily useful in the evaluation of theoretical predictions because it is sensitive to the formation of single packets. Thus, in the following examples both full and partial superrevivals appear as distinct peaks. However, fractional ones are less apparent. For this reason, we defer to Secs. IV B and

IV C comparison of the results of numerical computations with any details of our theory involving, for instance, the explicit values of the coefficients b_s.

As an example, consider the autocorrelation function for a Rydberg wave packet in hydrogen with $\bar{n}=319$ and $\sigma=2.5$. In this case, $\eta=79$, $\lambda=3$, and $t_{sr}\simeq 251$ μsec. The absolute square of the autocorrelation function is shown in Fig. 2. Figure 2(a) shows the behavior of the wave packet for the first 15 μsec. The first 1.2 μsec contains the cycle of fractional and full revivals shown in Fig. 1. This cycle collapses after approximately 5 μsec, whereupon new structure emerges. Figures 2(b) and 2(c) show $|A(t)|^2$ for times up to and just beyond $\frac{1}{6}t_{sr}$.

Our prediction for $q=6$ is that a single wave packet should form at $t\approx t_{frac}\simeq 41.4$ μsec. Only one wave packet appears because only one b_s coefficient is nonzero (see Sec. VI B). Equation (15) predicts the period of this packet as $T_{frac}\simeq 0.52$ μsec. In Fig. 2(c) we observe large peaks in $|A(t)|^2$ near 42 μsec, with a periodicity approximately equal to T_{frac}. These peaks are larger than the full-revival peak at $t\approx t_{rev}\simeq 1.05$ μsec. This is because at $t\simeq 41.4$ μsec the higher-order corrections to the time-dependent phase are contributing coherently to the wave function. Note also that between the large peaks at $t\simeq 41.4$ μsec there are smaller peaks with periodicities that are fractions of T_{frac}. These correspond to the formation of fractional revivals during the times between the periodic appearances of the full superrevival.

For $q=9$, the theory gives $t_{frac}\simeq 27.6$ μsec and $T_{frac}\simeq 0.35$ μsec. Figure 2(b) shows that the autocorrelation function exhibits peaks near this time, but with approximately half the period T_{frac}. This occurs because more than one subsidiary wave packet is forming, and they are unequally weighted. In this case, the fractional superrevival evolves into a partial superrevival at two separate times during each cycle.

The $q=12$ peaks at $t_{frac}\simeq 20.7$ μsec with $T_{frac}\simeq 0.26$ μsec are more pronounced than the $q=9$ peaks. This is because the corresponding subsidiary wave packets evolve into a structure with a single dominant wave packet, thereby creating large peaks in the autocorrelation function. The periodicity of the peaks agrees with the predicted value of T_{frac}.

No prominent peaks appear in Fig. 2(b) for $q=15$ at the times $t_{frac}\simeq 16.6$ μsec. As we show in Sec. IV B, in this case there are four unequally weighted subsidiary wave packets. These evidently do not evolve into a structure with one dominant wave packet.

Since $q=18$ is divisible by 9, the number of terms in the expansion of the wave function in this case is $l=q/3=6$. Of these six terms, three vanish. The remaining terms are unequally weighted with one of them substantially larger than the rest. This leads to the formation of a single packet at time $t_{frac}\simeq 13.8$ μsec, with a period $T_{frac}\simeq 0.17$ μsec. Figure 2(a) shows peaks in the autocorrelation function at this time with a periodicity that agrees with T_{frac}.

Peaks also appear in the autocorrelation function near $t\simeq 7$ μsec. For $q=36$, the theory gives $t_{frac}\simeq 6.91$ μsec and $T_{frac}\simeq 0.09$ μsec, which agrees with the observed periodicity. In this case, however, we find that there are 12 nonvanishing b_s coefficients that are unequal in magnitude. It is unclear why these subsidiary waves evolve into a partial superrevival.

B. Circular wave packets

This subsection examines more closely our theoretical description of circular Rydberg wave packets in hydrogen with $\bar{n}=319$ and $\sigma=2.5$. The time-dependent wave

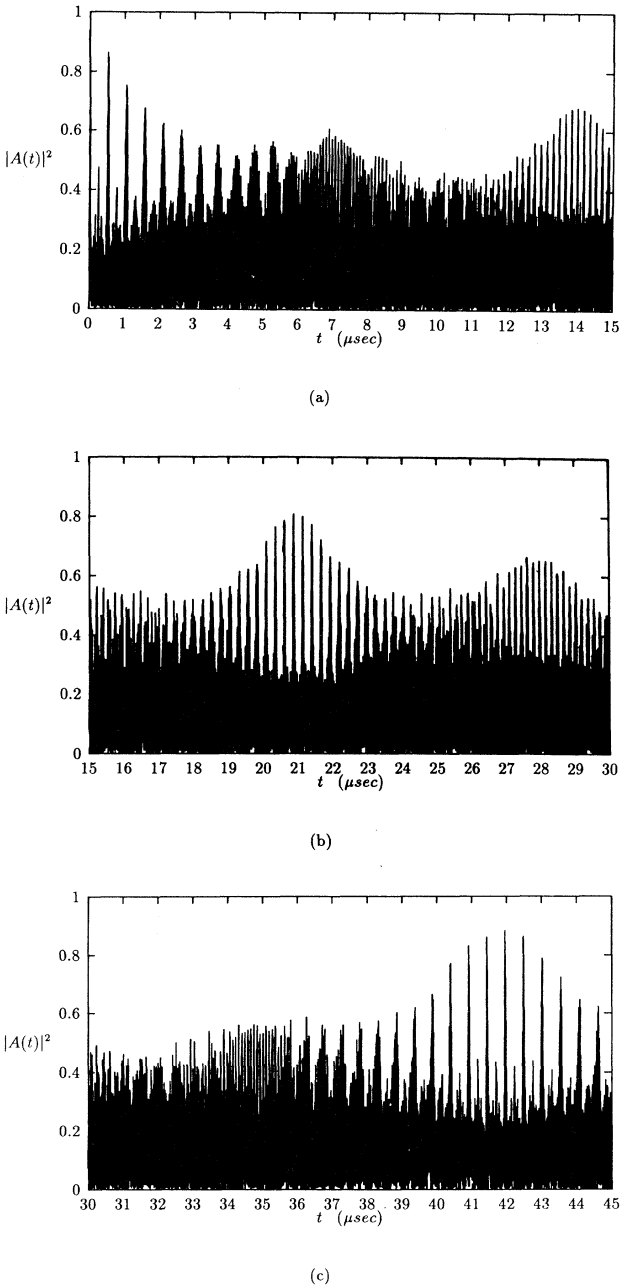

FIG. 2. The absolute square of the autocorrelation function for a hydrogenic Rydberg wave packet with $\bar{n}=319$ and $\sigma=2.5$ is plotted as a function of time in microseconds. (a) $t=0$–15 μsec, (b) $t=15$–30 μsec, and (c) $t=30$–45 μsec.

function is given analytically in Eq. (2) with the c_n coefficients specified by Eq. (3) and with $\varphi_n(\vec{r})=\psi_{n,n-1,n-1}(\vec{r})$. Plots of the wave packet at different times can be obtained numerically by taking advantage of the peaking of the c_n coefficients around the value $\bar{n}$. Figure 3 shows the azimuthal dependence at various times of a cross-sectional slice of the wave packet taken in the plane of the orbit and at fixed radius equal to the expectation value $\langle r \rangle = \frac{1}{2}\bar{n}(2\bar{n}+1)$.

The initial wave packet at time $t=0$ is presented in Fig. 3(a). It is localized about the azimuthal angle $\phi=0$. Figure 3(b) shows the first full revival, at time $t_{\rm rev}$. At this point, the packet has collapsed, passed through the sequence of fractional revivals, and reformed. It is primarily a single packet shifted in phase relative to the initial one, but some smaller subsidiary packets remain visible.

The remainder of the graphs in Fig. 3 shows the wave packet at times relevant for comparison with our theoretical analysis. In what follows, we give the b_s coefficients for the expansion (13) of the wave packet at the times $t_{\rm frac}$ for each of the cases $q=6$, 9, 12, 15, and 18. We also compare the packets at the times $t_{\rm frac}$ and $t_{\rm frac}+T_{\rm frac}$ to test the predicted periodicity. For $\bar{n}=319$, we have $\eta=79$ and $\lambda=3$. The value of l is given in Eq. (A4) and depends on q. The integer α that appears in the expansion of $\Psi(\vec{r},t)$ in Eq. (13) is equal to $8\eta/N$, where N is the product of all the factors of (8η) that are also factors of l. Note that we set the integer a in Eq. (A9) equal to 1. In fact, its value is irrelevant: if it changes, the b_s coefficients become permuted but leave unaffected the total sum of the subsidiary waves.

For $q=6$, we obtain $l=6$, $N=8$, $\alpha=79$, $t_{\rm frac}=\frac{1}{6}t_{\rm sr}-\frac{3}{8}t_{\rm rev}$, and $T_{\rm frac}=\frac{1}{2}t_{\rm rev}-\frac{5}{6}T_{\rm cl}$. Using Eq. (14), we find that $b_4=1$, while all the other b_s coefficients vanish. The wave function at $t_{\rm frac}$ can therefore be written as a single subsidiary packet. Since $\psi_{\rm cl}$ is periodic with period $T_{\rm cl}$, it is sufficient to evaluate the phase of $\psi_{\rm cl}(t_{\rm frac}+(s\alpha/l)T_{\rm cl})$ for $s=4\,\text{modulo}\,T_{\rm cl}$. Suppressing the $\vec{r}$ dependence, we find $\Psi(t_{\rm frac})\approx\psi_{\rm cl}(0)$. Figure 3(c) shows the wave packet at the time $t_{\rm frac}$. It does indeed consist of a single wave packet at the initial point in the orbital cycle. Comparing Fig. 3(c) to Fig. 3(b), which represents the wave packet at the full revival, we see that the full superrevival resembles the initial wave in Fig. 1(a) more closely than does the full revival at $t=t_{\rm rev}$. Moreover, the tail of subsidiary waves visible in Fig. 3(b) is absent in Fig. 3(c). The wave packet at the time $t_{\rm frac}+T_{\rm frac}$ is plotted in Fig. 3(d). This figure resembles Fig. 3(c), which verifies the predicted periodicity of the wave packet.

With $q=9$, we obtain $l=3$, $N=1$, $\alpha=632$, $t_{\rm frac}=\frac{1}{9}t_{\rm sr}-\frac{1}{4}t_{\rm rev}$, and $T_{\rm frac}=\frac{1}{3}t_{\rm rev}-\frac{8}{9}T_{\rm cl}$. In this case, there are three nonzero terms in the expansion of the wave function. We find

$$\Psi(t_{\rm frac})\approx b_0\psi_{\rm cl}(\tfrac{2}{9})+b_1\psi_{\rm cl}(\tfrac{8}{9})+b_2\psi_{\rm cl}(\tfrac{5}{9})\ , \tag{16}$$

where the argument of $\psi_{\rm cl}$ is written in units of $T_{\rm cl}$ and $|b_0|\simeq 0.45$, $|b_1|\simeq 0.85$, and $|b_2|\simeq 0.29$. This expansion predicts that the wave packet consists of three subsidiary packets. Since $\psi_{\rm cl}$ passes through the range $0-2\pi$ in ϕ at a constant rate, at a specified fractional interval in the cycle its angular position is at the corresponding fractional part of 2π. We therefore expect a large wave packet at $\phi\simeq\frac{8}{9}(2\pi)$, a medium one at $\phi\simeq\frac{2}{9}(2\pi)$, and a small one at $\phi\simeq\frac{5}{9}(2\pi)$. This prediction agrees with the plot in Fig. 3(e). The wave packet at the time $t_{\rm frac}+T_{\rm frac}$ is shown in Fig. 3(f). The periodicity $T_{\rm frac}$ of the wave packet is evident.

Since the wave function in this case has three distinct subsidiary wave packets, a large peak in the autocorrelation function is not to be expected. This is compatible with the structure of Fig. 2(b) at times near $t_{\rm frac}\simeq 27.6$ μsec. The appearance of peaks of equal height with a periodicity $\frac{1}{2}T_{\rm frac}$ indicates that the fractional superrevival is evolving into partial superrevivals twice each cycle, which is possible because the subsidiary wave packets are unequally weighted.

For $q=12$, we find $l=12$, $N=8$, $\alpha=79$, $t_{\rm frac}=\frac{1}{12}t_{\rm sr}-\frac{3}{16}t_{\rm rev}$, and $T_{\rm frac}=\frac{1}{4}t_{\rm rev}-\frac{5}{12}T_{\rm cl}$. The expansion of the wave packet yields

$$\Psi(t_{\rm frac})\approx b_1\psi_{\rm cl}(\tfrac{3}{4})+b_4\psi_{\rm cl}(\tfrac{1}{2})+b_7\psi_{\rm cl}(\tfrac{1}{4})+b_{10}\psi_{\rm cl}(0) \tag{17}$$

with $|b_1|=|b_4|=|b_7|=|b_{10}|\simeq\frac{1}{2}$. The remaining b_s coefficients vanish. The packet in this case consists of four equally weighted subsidiary packets evenly distributed in ϕ. Figure 3(g) confirms this prediction. However, there is some distortion, arising from higher-order terms neglected in our analysis. In Fig. 3(h) we plot the wave packet at time $t_{\rm frac}+T_{\rm frac}$. The periodicity is again evident.

For $q=15$, we have $l=15$, $N=1$, $\alpha=632$, $t_{\rm frac}=\frac{1}{15}t_{\rm sr}-\frac{3}{20}t_{\rm rev}$, and $T_{\rm frac}=\frac{1}{5}t_{\rm rev}-\frac{11}{15}T_{\rm cl}$. The expansion gives

$$\Psi(t_{\rm frac})\approx b_2\psi_{\rm cl}(\tfrac{2}{5})+b_5\psi_{\rm cl}(\tfrac{4}{5})+b_8\psi_{\rm cl}(\tfrac{1}{5})+b_{14}\psi_{\rm cl}(0)\ , \tag{18}$$

where the moduli of the complex coefficients are $|b_2|=|b_5|\simeq 0.45$, $|b_8|\simeq 0.72$, and $|b_{14}|\simeq 0.28$. For these values, we expect two equally weighted subsidiary wave packets at $\frac{2}{5}(2\pi)$ and $\frac{4}{5}(2\pi)$, a large subsidiary packet at $\frac{1}{5}(2\pi)$, and a small one at the origin. Figure 3(i) displays the packet at $t_{\rm frac}$. It agrees with the predictions. Figure 3(j) shows the wave packet at the time $t_{\rm frac}+T_{\rm frac}$, which again exhibits the expected periodicity.

Finally, in Fig. 3(k) we show the wave packet corresponding to $q=18$. Here, we obtain $l=6, N=8, \alpha=79, t_{\rm frac}=\frac{1}{18}t_{\rm sr}-\frac{1}{8}t_{\rm rev}$, and $T_{\rm frac}=\frac{1}{6}t_{\rm rev}-\frac{17}{18}T_{\rm cl}$. There are three nonzero coefficients b_s, so

$$\Psi(t_{\rm frac})\approx b_0\psi_{\rm cl}(\tfrac{1}{9})+b_2\psi_{\rm cl}(\tfrac{4}{9})+b_4\psi_{\rm cl}(\tfrac{7}{9})\ , \tag{19}$$

with $|b_0|\simeq 0.84$, $|b_2|\simeq 0.29$, and $|b_4|\simeq 0.45$. A large subsidiary wave packet is visible near $\frac{1}{9}(2\pi)$, an intermediate-sized one is near $\frac{7}{9}(2\pi)$, and a small one is near $\frac{4}{9}(2\pi)$, in agreement with the theoretical result. Fig-

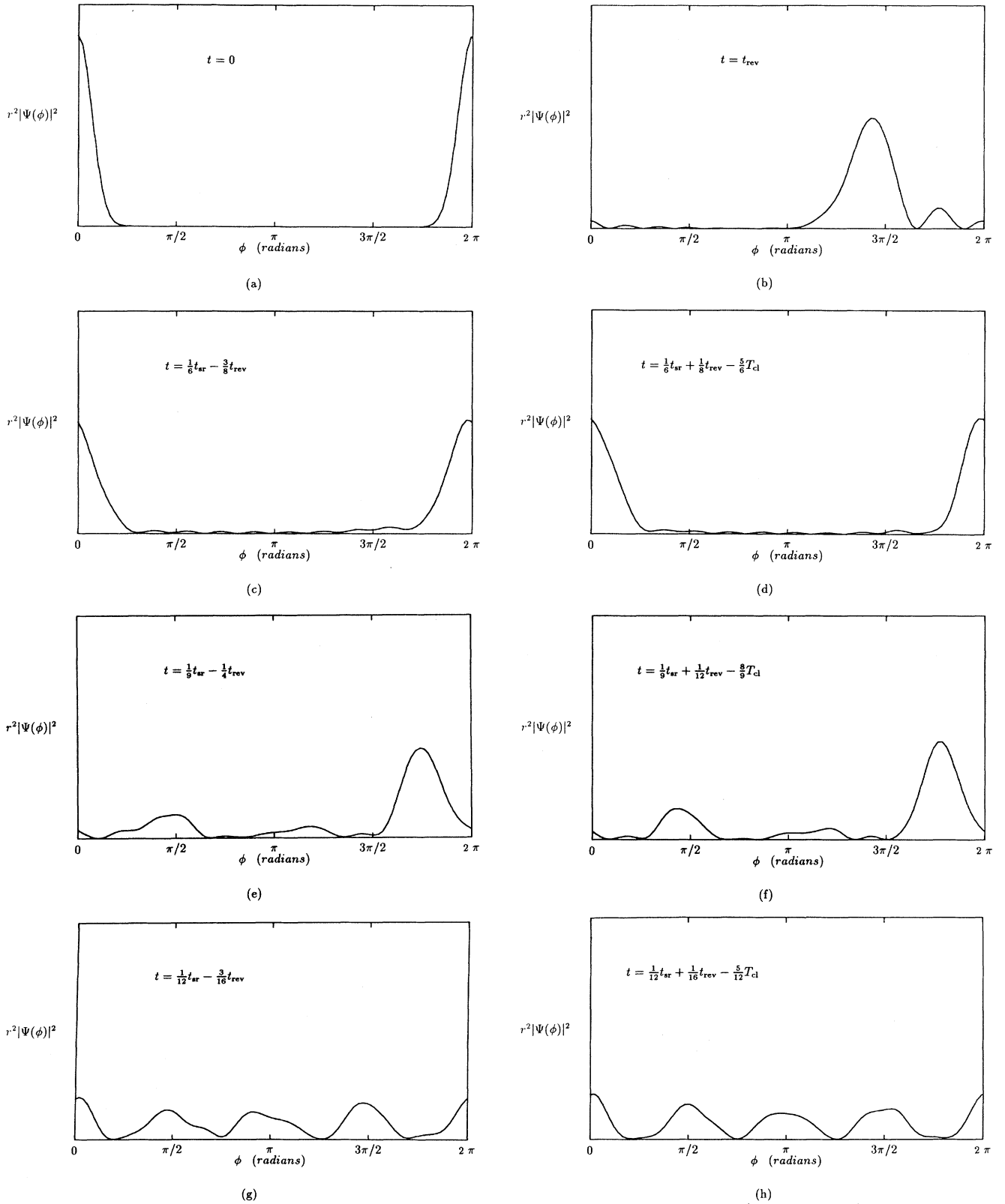

FIG. 3. Unnormalized circular wave packets for hydrogen with $\bar{n}=319$ and $\sigma=2.5$. Cross-sectional slices of the wave packet in the plane of the orbit and for $r=\langle r\rangle=\frac{1}{2}\bar{n}(2\bar{n}+1)$ are plotted as a function of the azimuthal angle ϕ in radians. (a) $t=0$, (b) $t=t_{\rm rev}$, (c) $t=\frac{1}{6}t_{\rm sr}-\frac{3}{8}t_{\rm rev}$, (d) $t=\frac{1}{6}t_{\rm sr}+\frac{1}{8}t_{\rm rev}-\frac{5}{6}T_{\rm cl}$, (e) $t=\frac{1}{9}t_{\rm sr}-\frac{1}{4}t_{\rm rev}$, (f) $t=\frac{1}{9}t_{\rm sr}+\frac{1}{12}t_{\rm rev}-\frac{8}{9}T_{\rm cl}$, (g) $t=\frac{1}{12}t_{\rm sr}-\frac{3}{16}t_{\rm rev}$, (h) $t=\frac{1}{12}t_{\rm sr}+\frac{1}{16}t_{\rm rev}-\frac{5}{12}T_{\rm cl}$, (i) $t=\frac{1}{15}t_{\rm sr}-\frac{3}{20}t_{\rm rev}$, (j) $t=\frac{1}{15}t_{\rm sr}+\frac{1}{20}t_{\rm rev}-\frac{11}{15}T_{\rm cl}$, (k) $t=\frac{1}{18}t_{\rm sr}-\frac{1}{8}t_{\rm rev}$, and (l) $t=\frac{1}{18}t_{\rm sr}+\frac{1}{24}t_{\rm rev}-\frac{17}{18}T_{\rm cl}$.

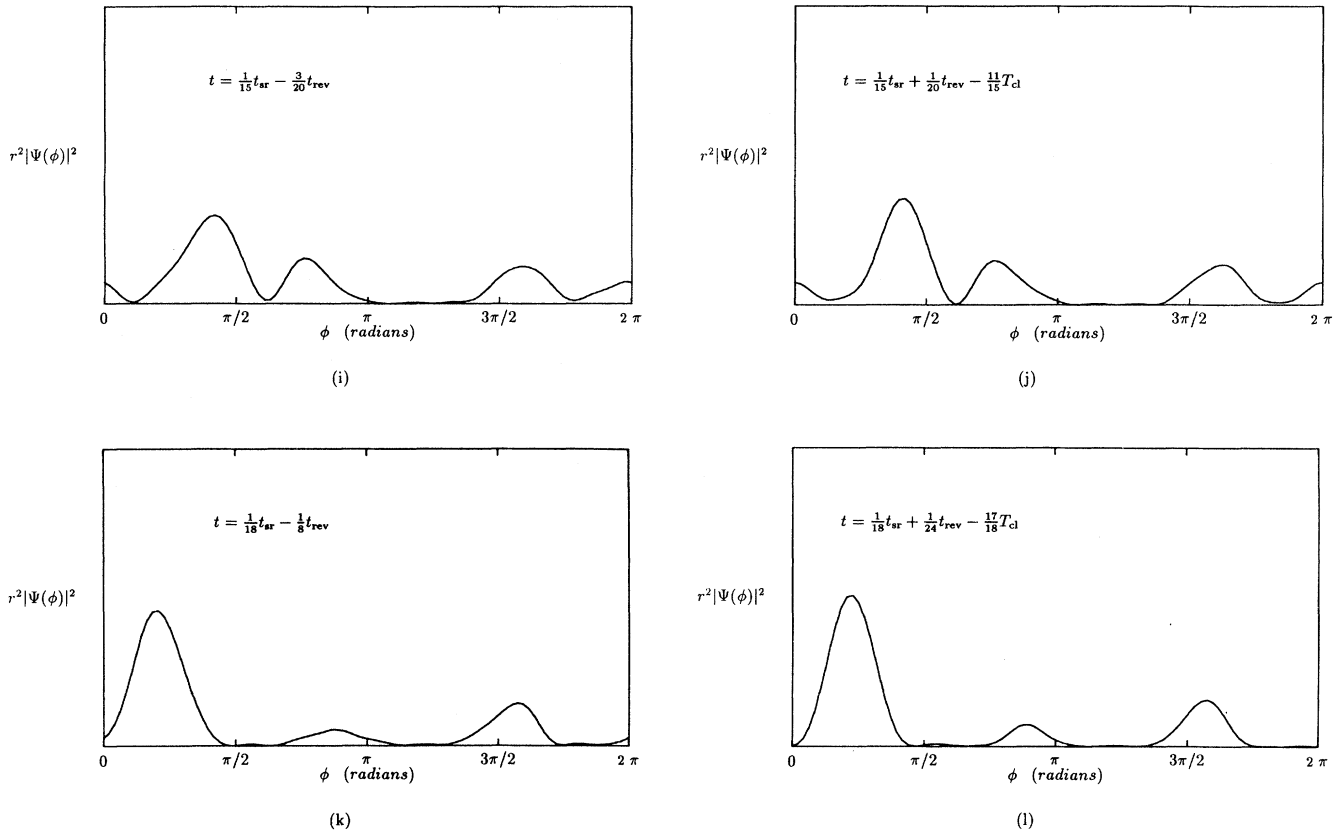

FIG. 3. (*Continued*).

ure 3(l) shows the wave packet at $t_{\rm frac}+T_{\rm frac}$, confirming that the periodicity is correctly given by $T_{\rm frac}$.

For $q>18$, more than four subsidiary wave packets appear in the expansion of the wave function at the times $t_{\rm frac}$. There are therefore fewer pronounced peaks in the autocorrelation function, and prominent partial superrevivals are less likely to form.

C. Radial wave packets

The previous sections have established the validity of our theory for the various types of superrevival. This subsection treats an example closely related to a feasible experimental situation: a p-state radial Rydberg wave packet for hydrogen with $\bar{n}=36$ and $\sigma=1.5$.

Figure 4(a) shows the plot of the radial wave packet at time $t=0$. The wave packet starts its cycle at the inner apsidal point and then moves radially to the outer apsidal turning point. Initially, the wave packet is highly oscillatory. As it moves, the packet changes shape in a way characteristic of a squeezed state [17]. In Fig. 4(b), we show the wave packet at the outer apsidal point at the time $\frac{1}{2}T_{\rm cl}$. Here, it is localized in the radial coordinate and is at its point of minimum uncertainty.

At the full revival, $t=t_{\rm rev}$, the wave packet has reformed after undergoing its cycle of collapse and fractional revivals and is located at its initial position near the inner apsidal point. For ease of comparison of the initial and full-revival packets, we show in Fig. 4(c) the full-revival packet displaced forward in time by $\frac{1}{2}T_{\rm cl}$. This brings it to the outer apsidal point where it is the most localized. The initial and full-revival packets are similar, although the latter has some distortion due to the higher-order corrections.

As before, the full superrevival is predicted to occur for $q=6$. This gives $l=6$, $N=72$, $\alpha=1$, $t_{\rm frac}=\frac{1}{6}t_{\rm sr}$, and $T_{\rm frac}=\frac{1}{2}t_{\rm rev}-\frac{1}{2}T_{\rm cl}$. Note that since $\bar{n}=36$ is divisible by 4, the fraction m/n in $t_{\rm frac}$ vanishes. The expansion of the wave function is $\Psi(t_{\rm frac})\approx b_4\psi_{\rm cl}(\frac{2}{3})$, with $b_4=1$ and all the other b_s coefficients vanishing. In this case, $\psi_{\rm cl}$ is a radial wave function, which in one complete cycle moves from the inner turning point to the outer one and back. At $t_{\rm frac}$, the wave function therefore represents a single packet two-thirds through the classical cycle. To compare this packet to the full revival, we view it displaced backward by $\frac{1}{6}T_{\rm cl}$ so it is at the outer turning point. Figure 4(d) shows the wave packet at this time. The full superrevival is visibly better localized than the full revival in Fig. 4(c), and it has less distortion. In Fig. 4(e), the wave packet is displayed one period $T_{\rm frac}$ later than the time of Fig. 4(d). Comparison shows that the packet has the predicted period $T_{\rm frac}$.

V. RYDBERG WAVE PACKETS IN ALKALI-METAL ATOMS

The previous sections of this paper have provided a satisfactory theory of the long-term behavior of Rydberg wave packets in hydrogen. However, the wave packets used to date in experiments to exhibit full and fractional revivals [8–12] have been produced in alkali-metal atoms. In the remainder of this paper, we show how to extend our previous theoretical analysis to these cases.

The Rydberg series for an alkali-metal atom is given by the energies

$$E_{n^*} = -\frac{1}{2n^{*2}} , \tag{20}$$

where $n^* = n - \delta(l)$ and $\delta(l)$ is an asymptotic quantum defect for an alkali-metal Rydberg atom. In what follows, we consider Rydberg wave packets in alkali-metal atoms that can be represented as a superposition of states strongly peaked around a central value $\bar{n}^* = \bar{n} - \delta(l)$ of the shifted principal quantum number. Following the simplification introduced at the end of Sec. II A, we assume that $\bar{n}$ is an integer. The extension of the results below to noninteger $\bar{n}$, along with the issue of disentangling laser detuning from features induced by quantum defects, has been considered in Ref. [26].

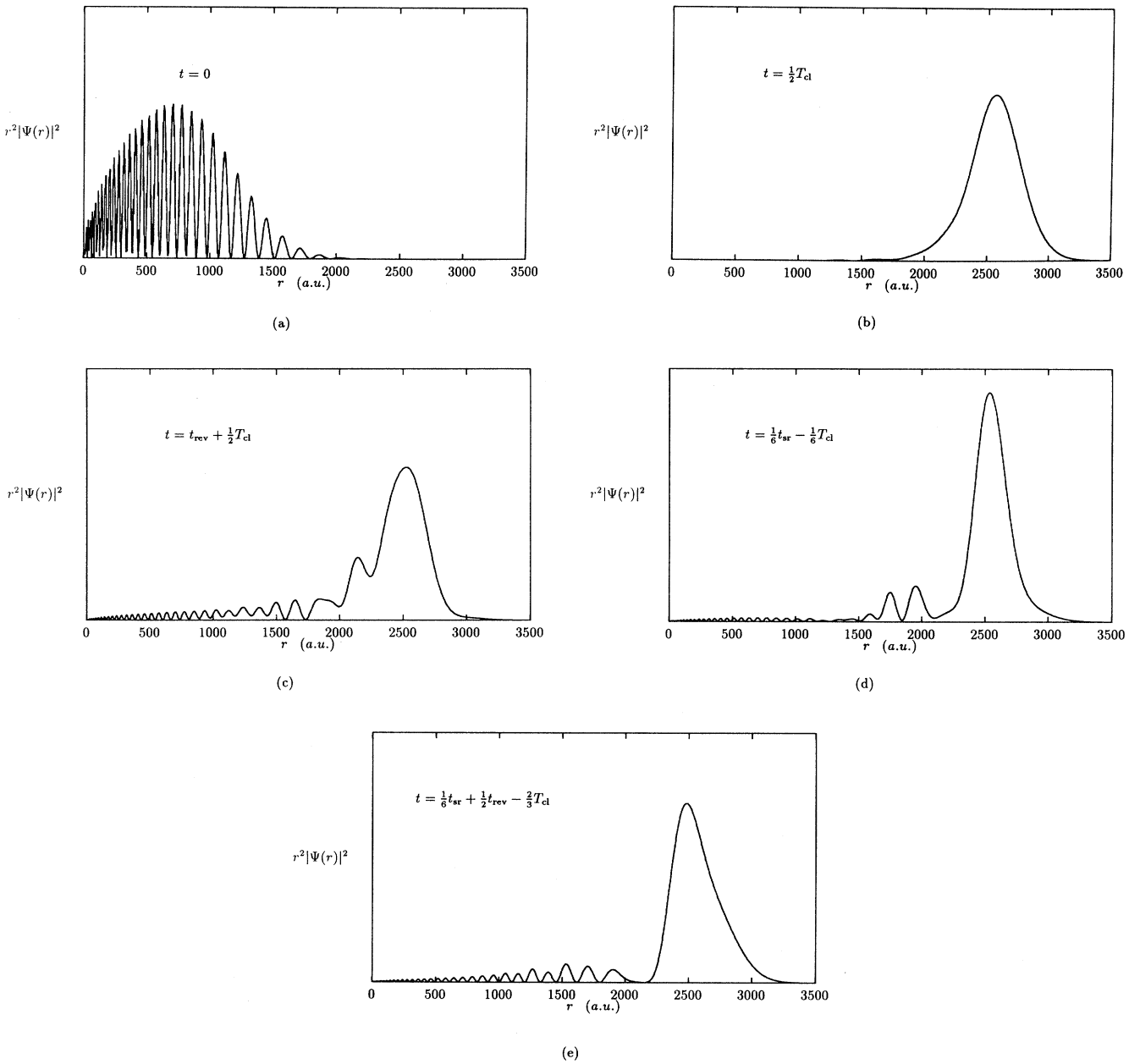

FIG. 4 Unnormalized radial wave packets for hydrogen with $\bar{n} = 36$ and $\sigma = 1.5$. The radial probability density is plotted as a function of r in atomic units. (a) $t = 0$, (b) $t = \frac{1}{2}T_{\rm cl}$, (c) $t = t_{\rm rev} + \frac{1}{2}T_{\rm cl}$, (d) $t = \frac{1}{6}t_{\rm sr} - \frac{1}{6}T_{\rm cl}$, and (e) $t = \frac{1}{6}t_{\rm sr} + \frac{1}{2}t_{\rm rev} - \frac{2}{3}T_{\rm cl}$.

We proceed by expanding the Rydberg energies as a Taylor series in n^*,

$$E_{n^*} \simeq E_{\bar{n}^*} + E'_{\bar{n}^*}(n-\bar{n}) + \tfrac{1}{2}E''_{\bar{n}^*}(n-\bar{n})^2 + \tfrac{1}{6}E'''_{\bar{n}^*}(n-\bar{n})^3 + \cdots . \quad (21)$$

The derivatives are taken with respect to n^*, and we have used the relation $(n^*-\bar{n}^*)=(n-\bar{n})$. The first three derivative terms define the time scales

$$T^*_{\rm cl} = 2\pi\bar{n}^{*3} , \quad (22)$$

$$t^*_{\rm rev} = \frac{2\bar{n}^*}{3} T^*_{\rm cl} , \quad (23)$$

and

$$t^*_{\rm sr} = \frac{3\bar{n}^*}{4} t^*_{\rm rev} , \quad (24)$$

which depend on the quantum defects.

Since the quantum defects $\delta(l)$ depend on l, we may no longer treat circular and radial wave packets generically. Circular wave packets have large values of l and so vanishing values of $\delta(l)$. A hydrogenic description therefore should be a good approximation for the analysis of the behavior of circular wave packets for alkali-metal atoms. In contrast, radial wave packets have small values of l. This means that their behavior is modified by the presence of quantum defects, with time scales and periodicities changed relative to those in hydrogen. In the following, we limit ourselves to considering radial wave packets, for which the quantum defects are important.

To incorporate nonhydrogenic features in our treatment, we use supersymmetry-based quantum-defect theory (SQDT), which has analytical wave functions with exact eigenvalues reproducing the Rydberg series for alkali-metal atoms [29]. This model describes the behavior of the valence electron in an alkali-metal atom as that of a single particle in an effective central potential. The effective potential is found by acting on the radial Coulomb potential for hydrogen with a supersymmetry transformation and then adding specific supersymmetry-breaking terms that incorporate electron-electron interactions and reproduce the Rydberg series while leaving the eigenfunctions analytical. A modified angular quantum number $l^*=l-\delta(l)+I(l)$ is introduced, where $I(l)$ is an integer playing the role of the supersymmetric shift. The resulting SQDT Hamiltonian is equivalent to one obtained by replacing n,l,E_n in the radial equation by n^*,l^*,E_{n^*}, respectively. The exact three-dimensional SQDT wave functions are $Y_{lm}(\theta,\phi)R_{n^*l^*}(r)$. These have the eigenenergies E_{n^*} given in Eq. (21) and form a complete and orthonormal set. More details on this model and references to the recent literature may be found in the review article [30].

Let us denote by $\varphi_{*n}(\vec{r})$ the eigenstates of an alkali-metal atom that are appropriate for the description of a radial wave packet. The analog of Eq. (1) for the wave function of the packet is then given by

$$\Psi(\vec{r},t) = \sum_{n=1}^{\infty} c_{n^*}\varphi_{*n}(\vec{r})\exp[-iE_{n^*}t] , \quad (25)$$

where the c_{n^*} are complex weights determined by the initial wave function. One role of SQDT in the analysis that follows is to provide explicit analytical expressions for the eigenstates in Eq. (25), i.e., we take $\varphi_{*n}(\vec{r})=Y_{lm}(\theta,\phi)R_{n^*l^*}(r)$.

Using the Taylor series (21), the wave function becomes

$$\Psi(\vec{r},t) = \sum_{k=-\infty}^{\infty} c_k\varphi_{*k}(\vec{r}) \times \exp\left[-2\pi i\left[\frac{kt}{T^*_{\rm cl}} - \frac{k^2t}{t^*_{\rm rev}} + \frac{k^3t}{t^*_{\rm sr}}\right]\right] . \quad (26)$$

We have kept the first three terms in the Taylor expansion so that times of order $t^*_{\rm sr}$ can be considered. The sum ranges over the integer values of $k=(n^*-\bar{n}^*)=(n-\bar{n})$. We assume that $\bar{n}^*$ is large so that the lower limit in the sum may be written as $-\infty$. Since k is integer valued, we can take the coefficients c_k as the Gaussian functions defined for hydrogen in Eq. (3).

We parametrize the times at which subsidiary wave packets form as

$$t^*_{\rm frac} = \frac{p}{q}t^*_{\rm sr} - \frac{m}{n}t^*_{\rm rev} , \quad (27)$$

where p and q are relatively prime integers, as are m and n. *A priori,* the integers p,q,m,n are unconstrained and, in particular, they are *not* related to the corresponding quantities for a hydrogenic radial wave packet.

Following the hydrogenic notation as closely as possible, we express $\bar{n}^*$ as

$$\bar{n}^* = 4\eta + \lambda - \frac{\mu}{\nu} , \quad (28)$$

where η,λ,μ,ν are all integer valued, $\lambda=0$, 1, 2, or 3, and μ/ν is an irreducible fraction less than one. In the most general case, μ/ν would represent the fractional part of a combination of the quantum defect and a laser detuning. In this paper, we assume the laser is on resonance, so μ/ν is the fractional part of the quantum defect. The effects of an additional laser detuning are described in Ref. [26]. Note that writing the quantum defect as an integer part minus a rational fraction of unity can always be done for experimentally determined quantum defects, which of necessity have only a finite accuracy.

We also define a wave function with time dependence involving only the linear term in k. In terms of $t^*_{\rm rev}$, it is

$$\psi_{\rm cl}(\vec{r},t) = \sum_{k=-\infty}^{\infty} c_k\varphi_{*k}(\vec{r})\exp\left[-2\pi i\frac{2\bar{n}^*}{3}\frac{kt}{t^*_{\rm rev}}\right] . \quad (29)$$

Note that at time zero, $\Psi(\vec{r},0)=\psi_{\rm cl}(\vec{r},0)$.

In Appendix C, we show that the phases induced by the shifts Δt in $\psi_{\rm cl}(\vec{r},t)$ have the same period as the higher-order contributions to the time-dependent phase in $\Psi(\vec{r},t)$ at the times $t^*_{\rm frac}$. It is therefore plausible to use the set $\psi_{\rm cl}(\vec{r},t^*_{\rm frac}+(s\alpha/l)T^*_{\rm cl})$ with $s=0,1,\ldots,l-1$ as a basis for an expansion of $\Psi(\vec{r},t^*_{\rm frac})$. We write

$$\Psi(\vec{r},t^*_{\rm frac})=\sum_{s=0}^{l-1} b_s \psi_{\rm cl}\left[\vec{r},t^*_{\rm frac}+\frac{s\alpha}{l}T^*_{\rm cl}\right] . \tag{30}$$

It is shown in Appendix C that the b_s coefficients have the same form as in Eq. (14) for hydrogen. The proof that this expansion is valid then follows as before, using Eq. (A11).

Equation (30) implies that the expansion in terms of subsidiary packets of a wave packet in an alkali-metal atom is similar to a corresponding one in hydrogen. In particular, the number of subsidiary wave packets that form at times $t^*_{\rm frac}$ and their relative proportions are the same as those in a corresponding wave packet in hydrogen at times $t_{\rm frac}$. However, the time scales $t^*_{\rm sr}$, $t^*_{\rm rev}$, and $T^*_{\rm cl}$ controlling the behavior are different from those in hydrogen, as are the times $t^*_{\rm frac}$ at which the expansion in subsidiary packets is valid.

In Appendix C, we determine the allowed values of $t^*_{\rm frac}$. We find that q must again be restricted to multiples of 3. The ratio m/n is given in Eq. (C2).

The proof that the wave packet and the absolute square of the autocorrelation function are periodic for times near $t^*_{\rm frac}$, with $p=1$, is also outlined in Appendix C. The allowed values of the period $T^*_{\rm frac}$ are found to be

$$T^*_{\rm frac}=\frac{3}{q}t^*_{\rm rev}-\frac{u}{v}T^*_{\rm cl} , \tag{31}$$

where the integers u and v are given in Eq. (C8).

A comparison of u/v for alkali-metal atoms [Eq. (C8) of Appendix C] with the corresponding definition for hydrogen [Eq. (B17) of Appendix B] reveals the appearance of an additional shift that depends on the fractional part μ/ν of $\bar{n}^*$. This means that the quantum defects cause an extra shift in the period $T^*_{\rm frac}$, in addition to the rescaling of $t_{\rm rev}$ and $T_{\rm cl}$. Note that if $\mu=0$, so that $\bar{n}^*$ is an integer, then the analysis reduces to the hydrogenic case.

To summarize, we have shown that a radial Rydberg wave packet in an alkali-metal atom forms superrevivals at times $t^*_{\rm frac}$ given by Eq. (27), where $p=1$, q is a multiple of 3, and the ratio m/n is determined. At these times, the wave function gathers into a finite number of subsidiary wave packets that move periodically with period $T^*_{\rm frac}$ given by Eq. (31) with a specified ratio u/v. The expressions for $t^*_{\rm frac}$ and $T^*_{\rm frac}$ differ from those for a corresponding wave packet in hydrogen by rescalings and shifts that depend on the quantum defect.

VI. EXAMPLES FOR RUBIDIUM

To illustrate in an experimentally viable scenario the long-term behavior of Rydberg wave packets when quantum defects are present, we consider in this section an example of a radial wave packet in rubidium with $\bar{n}=36$. For definiteness, we take p-state angular distributions, corresponding to the wave packets produced by a single short laser pulse. The example illustrates that full and fractional superrevivals may be observed for values of $\bar{n}$ corresponding to time delays currently accessible in experiments. Some other experimental issues are considered in Sec. VII.

In addition to providing a further check on the predictions of our theory, the long-term revival structure arising in this example can be compared to the analogous situation for hydrogen presented in Sec. IV C. For the autocorrelation function the behavior is generated from Eq. (9) with E_n replaced with E_{n^*}. For the radial wave packet itself, it is obtained from the analytical expression (25). We use a Gaussian distribution of width $\sigma=1.5$ for the weighting coefficients c_n, which makes it a good approximation to truncate the sum over the SQDT eigenstates after a finite number of terms.

The quantum defect for p states of rubidium is $\delta(1)\simeq 2.65$. This gives $\bar{n}^*\simeq 33.35$, $\eta=8$, $\lambda=2$, and $\mu/\nu=\frac{13}{20}$. The time scales determining the behavior of this packet are therefore $T^*_{\rm cl}\simeq 5.63$ psec, $t^*_{\rm rev}\simeq 0.12$ nsec, and $t^*_{\rm sr}\simeq 3.13$ nsec.

Figure 5 shows the absolute square of the autocorrelation function for this wave packet on time scales of order $\frac{1}{6}t^*_{\rm frac}$. The full revival peak is visible near $t^*_{\rm rev}$. For the relatively small value of $\bar{n}$ considered here, the revival structure is not as prominent as for larger values. Full and fractional superrevivals should nonetheless occur, albeit with less visible features. For $q=6$, our theoretical analysis predicts the occurrence of a full superrevival at $t^*_{\rm frac}\simeq 0.50$ nsec with periodicity $T^*_{\rm frac}\simeq 0.06$ nsec. Figure 5 contains peaks near $t^*_{\rm frac}$ in agreement with these values. The theory also predicts the appearance of fractional superrevivals for $q=9$ and 12 at the times $t^*_{\rm frac}\simeq 0.33$ and 0.25 nsec, respectively. The corresponding predicted periodicities are $T^*_{\rm frac}\simeq 0.04$ and 0.03 nsec. Peaks with appropriate periodicities may be observed near these times $t^*_{\rm frac}$ in Fig. 5.

Consider next the radial wave packet itself for this example. Figure 6 displays the packet at different times. The results should also be compared with the figures for the corresponding hydrogenic packet shown in Fig. 4.

The initial packet at time $t=0$ is displayed in Fig. 6(a). It is highly oscillatory and located near the inner apsidal point. Halfway through the classical orbit, at time $t=\frac{1}{2}T^*_{\rm cl}$, the wave function is radially localized and at its point of minimum uncertainty. See Fig. 6(b). The wave packet near the full revival time $t_{\rm rev}$ is shown in Fig. 6(c), after a time displacement by $\frac{4}{15}T^*_{\rm cl}$. This displacement

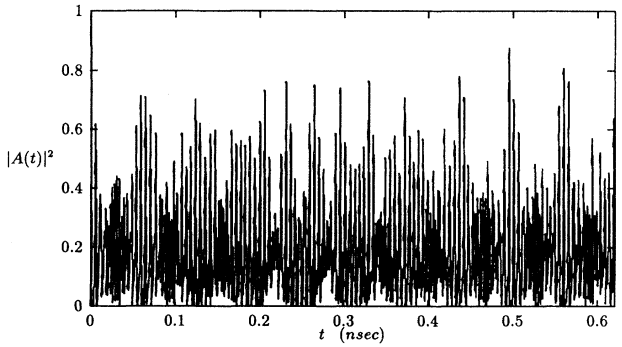

FIG. 5. The absolute square of the autocorrelation function for a Rydberg wave packet for rubidium with $\bar{n}=36$ and $\sigma=1.5$ is plotted as a function of time in nanoseconds. The p-state quantum defect is $\delta(1)=2.65$.

brings the packet to the outer apsidal point for ease of comparison.

The theoretical analysis suggests that a full superrevival occurs at $t^*_{\rm frac}=\frac{1}{6}t^*_{\rm sr}-\frac{27}{160}t^*_{\rm rev}$ with period $T^*_{\rm frac}=\frac{1}{2}t^*_{\rm rev}-\frac{37}{60}T^*_{\rm cl}$. The definition (14) of the b_s coefficients gives $b_1=1$, while the other b_s vanish. Evaluating the expansion (30) yields $\Psi(t_{\rm frac})\approx\psi_{\rm cl}(\frac{1}{10})$, where the argument of $\psi_{\rm cl}$ is written in units of $T^*_{\rm cl}$. For purposes of comparison at the outer apsidal point, we displace the packet by an additional amount $\frac{2}{5}T^*_{\rm cl}$. The result is shown in Fig. 6(d). A single wave packet appears, with less distortion than the full revival in Fig. 6(c).

In Fig. 6(e), the wave packet is displayed a time $T^*_{\rm frac}$ later than in Fig. 6(d). The wave packet is again at the outer apsidal point. The motion has period in agreement with $T^*_{\rm frac}$.

VII. DISCUSSION

In this paper, the behavior of Rydberg wave packets has been discussed on time scales large compared to the full-revival time $t_{\rm rev}$. We have demonstrated the appearance of various types of superrevival and have presented

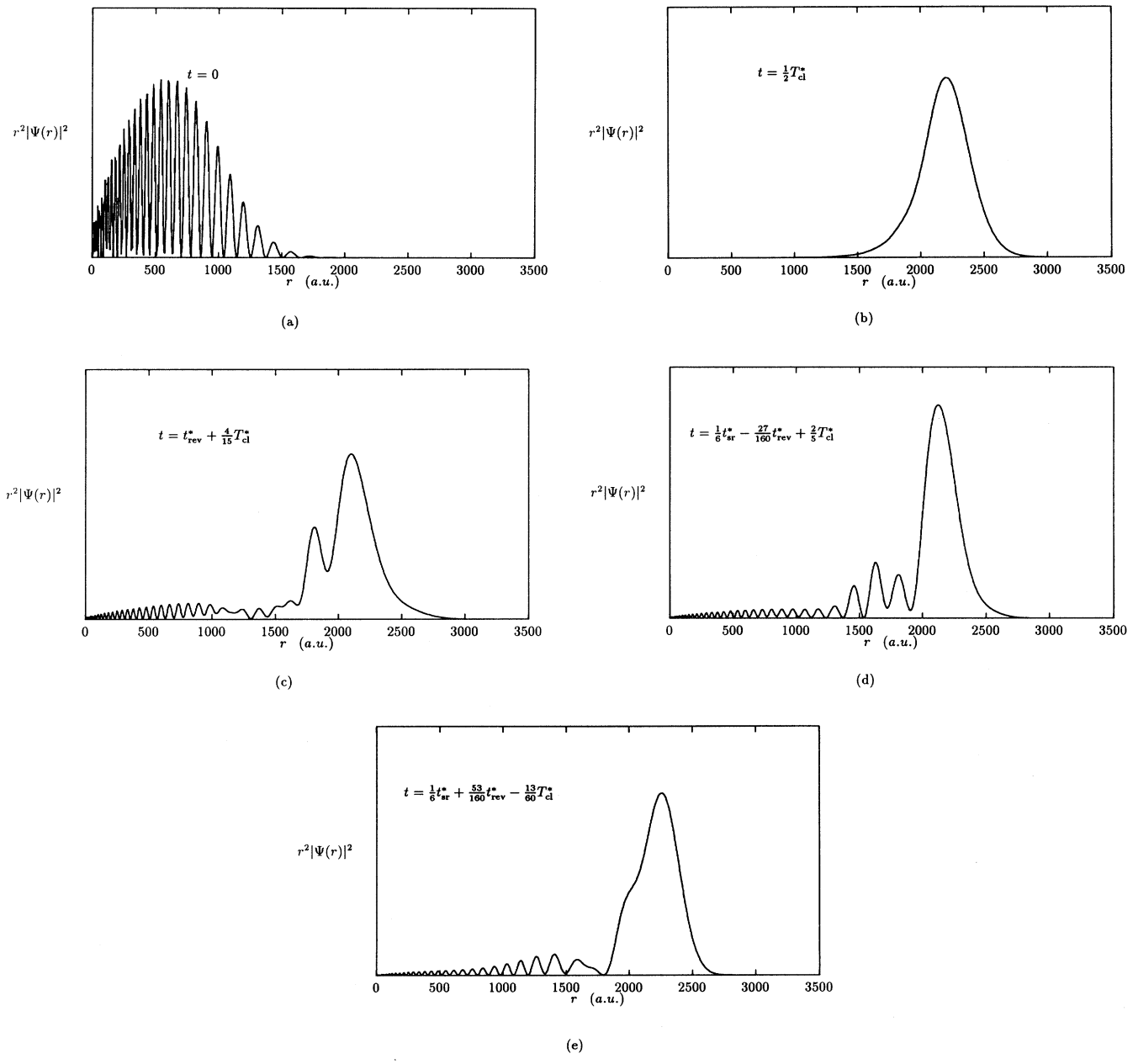

FIG. 6. Unnormalized radial wave packets for rubidium with $\bar{n}=36$ and $\sigma=1.5$. The p-state quantum defect is $\delta(1)=2.65$. The radial probability density is plotted as a function of r in atomic units. (a) $t=0$, (b) $t=\frac{1}{2}T^*_{\rm cl}$, (c) $t=t^*_{\rm rev}+\frac{4}{15}T^*_{\rm cl}$, (d) $t=\frac{1}{6}t^*_{\rm sr}-\frac{27}{160}t^*_{\rm rev}+\frac{2}{5}T^*_{\rm cl}$, and (e) $t=\frac{1}{6}t^*_{\rm sr}+\frac{53}{160}t^*_{\rm rev}-\frac{13}{60}T^*_{\rm cl}$.

a theoretical analysis that correctly predicts the times of formation, the associated periodicities, and their structure. Our analysis covers both hydrogenic Rydberg wave packets and the experimentally preferred Rydberg packets in alkali-metal atoms.

The fractional superrevivals that we present have long-term periodicities different from those of the usual fractional revivals. These periodicities could be observed for values of $\bar{n}$ corresponding to time delays in a pump-probe experiment of under 1 nsec.

When several packets form, we have shown that they often evolve quickly into a state where one packet is much larger than the others. In this case, large peaks appear in the autocorrelation function. All these features have been confirmed in numerically computed examples both for the autocorrelation function and for the wave packets themselves.

The wave-packet behavior on the time scale t_{sr} is self-similar in some ways to the fractional-revival structure appearing on the time scale t_{rev}. There are significant and experimentally observable differences, however. For example, the times t_{frac} are more restricted than the times at which the usual fractional revivals occur, since only times approximately given by certain irreducible fractions of $\frac{1}{3}t_{sr}$ are permitted. Moreover, the allowed periodicities T_{frac} are dominated by multiplies of $3t_{rev}$. The origin of the frequent appearance of multiples of three and 1/2 in our theory can be traced to the appearance of the third-order derivative of the energy in the original wave-packet expansion.

Our generalization of the hydrogenic analysis to include quantum defects uses a supersymmetry-based quantum-defect theory that provides a complete and orthonormal set of analytical wave functions with exact Rydberg eigenenergies. We have thereby proved that an expansion in terms of subsidiary packets is valid for a radial Rydberg packet in an alkali-metal atom. The controlling time scales T_{cl}, t_{rev}, and t_{sr} are modified relative to the hydrogenic case by quantum defects, as are the periodicities T_{frac} of the motion and the times t_{frac} at which the subsidiary-packet expansion is valid. Since the quantum defects for p states of the heavier alkali-metal atoms can be relatively large, these modifications can be significant and must be included in any accurate description of the evolution of the wave packet.

Relatively little prior literature exists on the long-term behavior of Rydberg wave packets. A long-term revival at $t=\bar{n}^3 T_{cl}$ has been presented in Ref. [1]. The time-dependent autocorrelation function (9) is an example of an almost-periodic function if the sum is truncated to a finite number of terms. Discussions of such functions exist in a more general context (see, for example, Ref. [31]). However, the wave function expansion (25) has a spatial dependence that is critical in the superrevival structure, involving the formation of the subsidiary wave packets. Reference [32] discusses a class of long-term revivals in hydrogen occurring when t and $\bar{n}$ are such that the energy expansion yields a phase that is an integer multiple of $2\pi i$. In contrast, the analysis of the full and fractional superrevivals presented here, which holds for arbitrary values of $\bar{n}$ in any alkali-metal atom, is based on finding the times t_{frac} when the phase in $\Psi(\vec{r},t)$ matches the phases of the shifted waves ψ_{cl} in the expansion. We find that at t_{frac} for $q=6$, corresponding to the full superrevival, the phase of the time-dependent terms is not necessarily an integer multiple of $2\pi i$. The point is that the superrevival times we find correspond to the formation of subsidiary wave packets. Unlike the usual fractional revivals, these are *not* equally weighted. The counterintuitive appearance of the $q=6$ superrevival occurs because all but one of the weighting coefficients b_s vanish.

In the remainder of this section, we discuss some issues relevant to the experimental verification of these results. Consider a pump-probe measurement utilizing either time-delayed photoionization or phase modulation with single-photon excitation, yielding a wave packet with a p-state angular distribution. In time-delayed photoionization, the packet evolves after formation for a delay time t, whereupon it interacts with a probe pulse ionizing the atom. In the phase-modulation technique, the wave packet is excited by two identical laser pulses separated in time by a delay t. The interference of the two wave packets produces an ionization signal proportional to their overlap.

Both these approaches permit measurement of an ionization signal displaying periodicities corresponding to the full and fractional revivals. References [10,11] describe the observation of a time-delayed photoionization signal for p-state radial wave packets in potassium for delay times up to approximately 800 psec. The measured ionization signal reveals both full and fractional revivals without any appreciable loss of the signal. Reference [33] uses the phase-modulation technique for wave packets of rubidium with $\bar{n}\simeq 46.5$ and 53.3. Fractional revivals with periodicities as small as $\frac{1}{7}T_{cl}$ have been resolved. However, there was a decay of the signal envelope with increasing delay, and the signal was quite small after 300 psec.

The limiting factor for the time delay in these experiments appears to be the ability to maintain a good overlap of the two laser pulses in the interaction region as the delay is increased. For Rydberg states with $\bar{n}=25-50$, transitions induced by interactions with blackbody radiation are not an issue in this context [27,34]. Although the Rydberg-state lifetimes induced by blackbody radiation are typically reduced by more than an order of magnitude compared to lifetimes induced by spontaneous emission, they are still several orders of magnitude more than the superrevival time scale t_{sr}. With a sufficiently low background pressure, transitions induced by collisional processes should not be a factor either.

The time-delayed photoionization experiments in Refs. [10,11] maintained a good signal for time delays of up to 800 psec. This is long enough to allow detection of both full and fractional superrevivals. In the example of rubidium with $\bar{n}=36$, considered in Sec. VI, t^*_{frac} for $q=6$ was found to be approximately 500 psec. Therefore, this full superrevival should be observable with existing experimental capabilities. The fractional superrevival at $t^*_{frac}\simeq 250$ psec with $T^*_{frac}\approx\frac{1}{4}t_{rev}$ should be measurable as

well.

As $\bar{n}$ is increased, the number of autocorrelation peaks increases and the fractional superrevivals become more prominent. Values of $\bar{n} \simeq 50$ would require a delay line of 3–4 nsec and the overlap of the laser pulses would have to be maintained for this amount of time. Assuming this can be achieved, the observation of the superrevival in this case would show the return to the near classical state of a quantum wave packet after a time of over 1200 classical orbits.

ACKNOWLEDGMENTS

R.B. thanks Colby College for a Science Division Grant. V.A.K. thanks the Aspen Center for Physics for hospitality during the initial stages of this work.

APPENDIX A

In this appendix, we show that at the times $t_{\rm frac}$ given in Eq. (10) the wave function $\Psi(\vec{r},t)$ can be expanded as a sum of subsidiary waves of the form $\psi_{\rm cl}(\vec{r},t)$, with t shifted by a fraction of the period $T_{\rm cl}$. Section A 1 analyzes the phase periodicity of $\Psi(\vec{r},t)$ at the times $t_{\rm frac}$, while Sec. A 2 obtains the phase periodicities of the subsidiary wave functions in the sum and matches them with the periodicity of $\Psi(\vec{r},t)$. We then examine the constraints on the times $t_{\rm frac}$ in Sec. A 3 and the properties of the expansion coefficients in Sec. A 4.

1. Phase of higher-order contributions in $\Psi(\vec{r},t)$

We first examine the periodicity at the times $t_{\rm frac}$ of the phase of the full wave function $\Psi(\vec{r},t)$. We are interested in the terms of higher order in k in Eq. (8) that result from the expansion of the energy in a Taylor series.

Substituting the expression for $t_{\rm frac}$ in Eq. (10) into $\Psi(\vec{r},t)$ and neglecting terms in the exponential of order $t_{\rm rev}/t_{\rm sr} \ll 1$, we find that the second- and the third-order terms in the energy lead to a phase factor $\exp[2\pi i\theta_k]$, where

$$\theta_k = \frac{3\bar{n}p}{4q}k^2 - \frac{m}{n}k^2 - \frac{p}{q}k^3 . \tag{A1}$$

We wish to find the minimum period l for shifts in k that leaves the phase $\exp[2\pi i\theta_k]$ invariant.

The analysis is simplified if we first impose a condition on m/n to reduce the general case to the same form as the one with $\bar{n}$ divisible by 4. The definition for $\bar{n}$ in Eq. (11) suggests we impose

$$\frac{m}{n} = \frac{3\lambda p}{4q} \pmod 1 , \tag{A2}$$

which simplifies the expression for θ_k in the general case. The relatively prime integers m and n obeying Eq. (A2) are then specified once the right-hand side of Eq. (A2) has been fully reduced.

The choice (A2) leads to a simplified form of the phase:

$$\theta_k = \frac{3\eta p}{q}k^2 - \frac{p}{q}k^3 . \tag{A3}$$

Define l as the minimum period in k that leaves θ_k invariant (mod 1), i.e., l is the smallest integer satisfying $\theta_{k+l} = \theta_k \pmod 1$. Then, there are two possible solutions for l, both dependent on q:

$$l = \begin{cases} q & \text{if } q/9 \neq 0 \pmod 1 \\ q/3 & \text{for } q/9 = 0 \pmod 1 . \end{cases} \tag{A4}$$

2. Phase of the subsidiary waves $\psi_{\rm cl}(\vec{r},t)$

The second phase of interest results when the macroscopically distinct subsidiary waves $\psi_{\rm cl}$ are shifted in time. We next evaluate the periodicity of this phase and match it to the one obtained above for $\Psi(\vec{r},t)$.

Consider a shift Δt in time of the classical wave function $\psi_{\rm cl}(\vec{r},t)$ defined in Eq. (12). We take a shift of the form

$$\Delta t = \frac{a}{b}t_{\rm rev} + \frac{c}{d}T_{\rm cl} , \tag{A5}$$

where a and b are relatively prime integers, as are c and d. This shift generates a phase factor $\exp[-2\pi i\phi_k]$ in $\psi_{\rm cl}(\vec{r},t)$, where

$$\phi_k = \frac{2\bar{n}a}{3b}k + \frac{c}{d}k . \tag{A6}$$

To simplify this expression, we choose the relatively prime integers c and d to satisfy

$$\frac{2\lambda a}{3b} + \frac{c}{d} = 0 \pmod 1 , \tag{A7}$$

where the first term is understood to be fully reduced. The phase ϕ_k then reduces to

$$\phi_k = \frac{8\eta a}{3b}k . \tag{A8}$$

To write the full wave function as an expansion in the subsidiary waves, the two sets of phases must have the same periodicity. We therefore impose the condition that the phase ϕ_k be periodic in k with the same minimum value l as the period of the phase θ_k in $\Psi(\vec{r},t)$. This requirement can be satisfied by an appropriate reduction of the fractional coefficient of k in Eq. (A8). It implies that we can write

$$\frac{8\eta a}{3b} = \frac{\alpha N}{lN} = \frac{\alpha}{l} . \tag{A9}$$

The integer N is the product of all factors of $8\eta a$ that are also factors of l, and $\alpha = 8\eta a/N$ is also an integer. Since α contains no factors that are also factors of l, α and l are relatively prime. With this reduction, $\phi_k = \alpha k/l$. The minimum period for k in ϕ_k is therefore l, as desired.

With the choices for c and d in Eq. (A7) and the reduction of $8\eta a/3b$ in Eq. (A9), we find that the time shifts Δt in $\psi_{\rm cl}(\vec{r},t)$ become

$$\Delta t = \frac{\alpha}{l}T_{\rm cl} . \tag{A10}$$

3. Constraints on $t_{\rm frac}$

The expansion of the wave function $\Psi(\vec{r},t)$ in terms of the shifted wave functions $\psi_{\rm cl}$ is given in Eq. (13), and the

b_s coefficients are defined in Eq. (14). The time of formation of the subsidiary wave packets are the times $t_{\rm frac}$ given by Eq. (10). The integers m and n must satisfy Eq. (A2). We next prove that l and hence q must be a multiple of 3.

Examining the reduction of the ratio in Eq. (A9), we see that the integer b satisfies the condition $b=lN/3$. Since all the factors of N are also factors of l, the only way that b can be an integer is if l (and hence N as well) is a multiple of 3. Therefore, the allowed values of l must all be multiples of 3. Since l is given in Eq. (A4) either as q for $q/9\neq 0$ (mod 1) or as $q/3$ for $q/9=0$ (mod 1), it follows that q must also be a multiple of 3.

It turns out that the analysis of the wave-packet and the autocorrelation-function periodicities given in Appendix B yields the further constraint $p=1$. We therefore have the constraints on the times $t_{\rm frac}$ given by Eq. (10) that q must be a multiple of 3, $p=1$, and m/n obeys Eq. (A2).

4. Properties of b_s coefficients

The form of the complex coefficients b_s multiplying the subsidiary wave functions $\psi_{\rm cl}$ at the times $t_{\rm frac}$, given in Eq. (14), reduces the expansion (13) to an identity. Substitute Eq. (14) into the expansion (13) for $\Psi(\vec{r},t)$ at the times $t_{\rm frac}$ and use the identity

$$\frac{1}{l}\sum_{s=0}^{l-1}\left[\exp\left[-2\pi i\frac{\alpha(k-k')}{l}\right]\right]^s = (\delta_{k,k'}+\delta_{k,k'\pm l}+\cdots)\ . \quad \text{(A11)}$$

This yields the expression in Eq. (8) at times $t\approx t_{\rm frac}$, up to terms in the exponential of order $t_{\rm rev}/t_{\rm sr}\ll 1$.

Note that the identity (A11) holds only if α and l are relatively prime. This means that the reduction of the ratio of integers in Eq. (A9) is a necessary condition for the formation of the subsidiary wave packets at the time $t_{\rm frac}$. Moreover, as discussed in Sec. A 3, it leads to the restriction that q must be a multiple of 3.

If we multiply the expansion for b_s in Eq. (14) by its complex conjugate, sum over s, and use the identity in Eq. (A11), we get

$$\sum_{s=0}^{l-1}|b_s|^2=1\ . \quad \text{(A12)}$$

This implies that the normalization of the wave function is maintained at the times $t_{\rm frac}$, as expected.

APPENDIX B

In this appendix, we examine the periodicities of the wave packet and the autocorrelation function. Section B 1 contains the proof that the wave packet $|\Psi(\vec{r},t)|^2$ is periodic at times $t\approx t_{\rm frac}$, with a period $T_{\rm frac}$ that depends on $t_{\rm rev}$ and $T_{\rm cl}$. Section B 2 contains the corresponding analysis for the autocorrelation function.

1. Periodicity of the wave packet

The wave function $\Psi(\vec{r},t)$ through third order in the energy expansion is given at the times $t_{\rm frac}$ by Eq. (8). The issue of its periodicity can be addressed by considering the effect of shifting the time,

$$t_{\rm frac}\rightarrow t_{\rm frac}+\frac{e}{f}t_{\rm rev}\ , \quad \text{(B1)}$$

where e and f are integers.

We are interested in the smallest possible value of e/f that leads to periodicity in $\Psi(\vec{r},t)$. The appearance of periodic structures in $\Psi(\vec{r},t)$ upon time shifts of the form (B1) is possible only if the minimum periodicity of k in θ_k [cf. Eq. (A3)] remains l *and* if the ensuing modified coefficients in the expansion (13) can be expressed in terms of the original coefficients b_s. We have performed an analysis for arbitrary e and f along the lines of what follows in this subsection, from which we have shown that the minimum value of e/f is

$$\frac{e}{f}=\frac{3}{q}\ . \quad \text{(B2)}$$

For simplicity in what follows, we restrict our treatment here to this explicit value.

Under the shift given by Eqs. (B1) and (B2), the phase θ_k of the higher-order time-dependent terms in $\Psi(\vec{r},t)$ becomes

$$\theta'_k=\frac{3(\eta p+1)}{q}k^2-\frac{p}{q}k^3\ , \quad \text{(B3)}$$

where we have kept terms only up to order $t_{\rm rev}/t_{\rm sr}\ll 1$. This phase continues to have the same minimum period l under changes in the summation index k as did the phase θ_k, i.e., $\theta'_{k+l}=\theta'_k$ for the same values of l as in Eq. (A4).

Next, consider the expansion of $\Psi(\vec{r},t_{\rm frac}+(3/q)t_{\rm rev})$ as a sum of subsidiary wave functions $\psi_{\rm cl}$ at the time $t_{\rm frac}+(3/q)t_{\rm rev}$:

$$\Psi\left[\vec{r},t_{\rm frac}+\frac{3}{q}t_{\rm rev}\right] = \sum_{s=0}^{l-1}b'_s\psi_{\rm cl}\left[\vec{r},t_{\rm frac}+\left[\frac{2\bar{n}}{q}+\frac{s\alpha}{l}\right]T_{\rm cl}\right]\ . \quad \text{(B4)}$$

In this equation, we have used the replacement $(3/q)t_{\rm rev}=(2\bar{n}/q)T_{\rm cl}$, and the b'_s are complex coefficients given by

$$b'_s=\frac{1}{l}\sum_{k'=0}^{l-1}\exp\left[2\pi i\frac{\alpha s}{l}k'\right]\exp[2\pi i\theta'_{k'}]\ . \quad \text{(B5)}$$

These coefficients are the same as those of Eq. (14) but with $\theta_k\rightarrow\theta'_k$.

We next show that the set of coefficients b'_s in Eq. (B5) can be found in terms of the previous set b_s, which are defined in Eq. (14). First, we let $k'\rightarrow k'-1$ in the definition of b'_s. We get

$$b_s' = \exp\left[2\pi i\frac{\alpha s}{l}\right]\exp\left[2\pi i\frac{3(\eta p+1)}{q}\right]\exp\left[-2\pi i\frac{p}{q}\right] \times\frac{1}{l}\sum_{k=-1}^{l-2}\exp\left[2\pi i\frac{\alpha s}{l}k\right]\exp\left[2\pi i\left[\frac{3(\eta p+1)-3p}{q}k^2-\frac{p}{q}k^3\right]\right]\exp\left[2\pi i\left[\frac{6(\eta p+1)}{q}-\frac{3p}{q}\right]k\right]. \quad \text{(B6)}$$

If we require that $p=1$, then

$$\exp\left[2\pi i\left[\frac{3(\eta p+1)-3p}{q}k^2-\frac{p}{q}k^3\right]\right]=\exp[2\pi i\theta_k], \quad \text{(B7)}$$

where θ_k is defined in Eq. (A3). We then define a quantity J as

$$J=\begin{cases}3 & \text{if } q/9\neq 0 \pmod 1\\ 1 & \text{if } q/9=0 \pmod 1,\end{cases} \quad \text{(B8)}$$

which permits us to write $q=3l/J$. This gives

$$b_s' = \exp\left[2\pi i\frac{\alpha s}{l}\right]\exp\left[2\pi i\frac{3(\eta+1)}{q}\right]\exp\left[-2\pi i\frac{1}{q}\right] \times\frac{1}{l}\sum_{k=-1}^{l-2}\exp[2\pi i\theta_k] \times\exp\left[2\pi i\left[\frac{\alpha s}{l}+\frac{J(2\eta+1)}{l}\right]k\right]. \quad \text{(B9)}$$

The quantity $J(2\eta+1)/l$ can be written as $\alpha x/l$ provided an integer x exists that satisfies

$$\alpha x = J(2\eta+1) \pmod l. \quad \text{(B10)}$$

It can be shown that an integer-valued equation of this form has a solution x if the greatest common divisor of α and l divides evenly into $J(2\eta+1)$. Since α and l are relatively prime, their greatest common divisor is 1, and this divides evenly into $J(2\eta+1)$. Thus, there always exists an integer x that satisfies Eq. (B10), and we may replace $[\alpha s+J(2\eta+1)]/l$ by $\alpha(s+x)/l$.

Since the exponential factors inside the sum (B9) are periodic with period l, we can shift the summation over k back to the range $k=0$ to $l-1$. We then obtain

$$b_s' = \exp\left[2\pi i\frac{\alpha s}{l}\right]\exp\left[2\pi i\frac{3(\eta+1)}{q}\right] \times\exp\left[-2\pi i\frac{1}{q}\right]b_{(s+x)_{\mathrm{mod}\,l}}. \quad \text{(B11)}$$

Defining the phase factor

$$\exp[2\pi i\Theta_s]=\exp\left[2\pi i\frac{\alpha s}{l}\right]\exp\left[2\pi i\frac{3(\eta+1)}{q}\right] \times\exp\left[-2\pi i\frac{1}{q}\right], \quad \text{(B12)}$$

we then have, for $p=1$, that the coefficients b_s' are given by

$$b_s' = \exp[2\pi i\Theta_s]b_{(s+x)_{\mathrm{mod}\,l}}, \quad \text{(B13)}$$

where x is a given integer. From this it follows that $|b_s'|=|b_{(s+x)_{\mathrm{mod}\,l}}|$. We use this relation to prove that the motion of the wave packet is periodic.

The probability density for the wave packet at the time $t_{\mathrm{frac}}+(3/q)t_{\mathrm{rev}}$ is the absolute square of the expression (B4). Since the subsidiary wave packets are by construction localized in space and distributed evenly along the orbit, they have little or no overlap. This permits us to ignore the cross terms in the absolute square of the wave function. Substituting the expression (B13) for b_s' into Eq. (B4) and taking the absolute square gives

$$\left|\Psi\left[\vec{r},t_{\mathrm{frac}}+\frac{3}{q}t_{\mathrm{rev}}\right]\right|^2 =\sum_{s=0}^{l-1}|b_{(s+x)_{\mathrm{mod}\,l}}|^2 \times\left|\psi_{\mathrm{cl}}\left[\vec{r},t_{\mathrm{frac}}+\left[\frac{2\bar{n}}{q}+\frac{s\alpha}{l}\right]T_{\mathrm{cl}}\right]\right|^2. \quad \text{(B14)}$$

Since the integer x always exists, we can set $s'=(s+x)_{\mathrm{mod}\,l}$ and reorder the terms to get

$$\left|\Psi\left[\vec{r},t_{\mathrm{frac}}+\frac{3}{q}t_{\mathrm{rev}}\right]\right|^2 =\sum_{s'=0}^{l-1}|b_{s'}|^2\left|\psi_{\mathrm{cl}}\left[\vec{r},t_{\mathrm{frac}}+\left[\frac{2\bar{n}}{q}-\frac{\alpha x}{l}\right]T_{\mathrm{cl}}+\frac{\alpha s'}{l}T_{\mathrm{cl}}\right]\right|^2. \quad \text{(B15)}$$

Introduce the irreducible ratio u/v of integers u and v satisfying

$$\frac{u}{v}=\frac{2\bar{n}}{q}-\frac{\alpha x}{l} \pmod 1. \quad \text{(B16)}$$

Using Eq. (11) of Sec. III A and Eqs. (B8) and (B10), this definition of u/v may be rewritten as

$$\frac{u}{v}=\frac{2(\eta+\lambda)-3}{q} \pmod 1. \quad \text{(B17)}$$

Equation (B15) then becomes

$$\left|\Psi\left[\vec{r},t_{\mathrm{frac}}+\frac{3}{q}t_{\mathrm{rev}}\right]\right|^2=\left|\Psi\left[\vec{r},t_{\mathrm{frac}}+\frac{u}{v}T_{\mathrm{cl}}\right]\right|^2, \quad \text{(B18)}$$

where we have used Eq. (13) and the assumption that the subsidiary wave packets do not overlap.

Since $T_{\mathrm{cl}}\ll t_{\mathrm{rev}}$, the expansion in Eq. (13) holds for shifts in time of order T_{cl}. We may therefore subtract

$(u/v)T_{\rm cl}$ from t on both sides of Eq. (B18) to obtain

$$\left|\Psi\left[\vec{r},t_{\rm frac}+\frac{3}{q}t_{\rm rev}-\frac{u}{v}T_{\rm cl}\right]\right|^2=|\Psi(\vec{r},t_{\rm frac})|^2\ . \quad \text{(B19)}$$

Finally, we can define the period $T_{\rm frac}$ as in Eq. (15), where the integers u and v satisfy Eq. (B17).

We have thus proved that at the times $t\approx t_{\rm frac}$, the wave packet is periodic with the period $T_{\rm frac}$.

2. Periodicity of the autocorrelation function

A similar method can be used to show that at the times $t_{\rm frac}$ the absolute square of the autocorrelation function is periodic with the same period $T_{\rm frac}$. The autocorrelation function at time $t_{\rm frac}$ is $A(t_{\rm frac})=\langle\Psi(\vec{r},0)|\Psi(\vec{r},t_{\rm frac})\rangle$. The initial wave function $\Psi(\vec{r},0)$ is $\psi_{\rm cl}(\vec{r},0)$. Shifting $t_{\rm frac}$ to $t_{\rm frac}+(3/q)t_{\rm rev}$ and using Eqs. (B4) and (B13) and the definition of u/v in Eq. (B17) yields

$$A\left[t_{\rm frac}+\frac{3}{q}t_{\rm rev}\right]=\sum_{s'=0}^{l=1}\exp[2\pi i\Theta_{s'}]b_{s'}\left\langle\psi_{\rm cl}(0)\left|\psi_{\rm cl}\left[t_{\rm frac}+\frac{u}{v}T_{\rm cl}+\frac{\alpha s'}{l}T_{\rm cl}\right]\right\rangle\right., \quad \text{(B20)}$$

where we have suppressed the $\vec{r}$ dependence. The phase $\exp[2\pi i\Theta_{s'}]$ is given in Sec. B 1. Note that the substitution $s'=(s+x)_{{\rm mod}\,l}$ has been made.

Taking the absolute square of $A(t_{\rm frac}+(3/q)t_{\rm rev})$ gives

$$\begin{aligned}\left|A\left[t_{\rm frac}+\frac{3}{q}t_{\rm rev}\right]\right|^2=&\sum_{s'=0}^{l-1}|b_{s'}|^2\left|\left\langle\psi_{\rm cl}(0)\left|\psi_{\rm cl}\left[t_{\rm frac}+\frac{u}{v}T_{\rm cl}+\frac{\alpha s'}{l}T_{\rm cl}\right]\right\rangle\right|^2\\&+\sum_{\substack{s,s'=0\\ s\neq s'}}^{l-1}\exp[2\pi i(\Theta_{s'}-\Theta_s)]b_{s'}b_s^*\left\langle\psi_{\rm cl}\left[t_{\rm frac}+\frac{u}{v}T_{\rm cl}+\frac{\alpha s}{l}T_{\rm cl}\right]\left|\psi_{\rm cl}(0)\right\rangle\right.\\&\times\left\langle\psi_{\rm cl}(0)\left|\psi_{\rm cl}\left[t_{\rm frac}+\frac{u}{v}T_{\rm cl}+\frac{\alpha s'}{l}T_{\rm cl}\right]\right\rangle\right.. \quad \text{(B21)}\end{aligned}$$

The first term on the right-hand side is just $|A(t_{\rm frac}+(u/v)T_{\rm cl})|^2$. Since $s\neq s'$ in the second term and since we assume that the subsidiary wave functions do not overlap appreciably, one of the inner products in the double sum must vanish. We can therefore neglect this term.

Subtracting $(u/v)T_{\rm cl}$ from both sides produces

$$\left|A\left[t_{\rm frac}+\frac{3}{q}t_{\rm rev}-\frac{u}{v}T_{\rm cl}\right]\right|^2=|A(t_{\rm frac})|^2\ . \quad \text{(B22)}$$

This proves that the square of the autocorrelation function is periodic at the times $t_{\rm frac}$ with period $T_{\rm frac}$ given by Eq. (15).

APPENDIX C

In this appendix, we prove that at the times $t^*_{\rm frac}$ the SQDT wave packet $\Psi(\vec{r},t)$ for an alkali-metal atom can be written as an expansion over subsidiary packets $\psi_{\rm cl}(\vec{r},t)$. In analogy with the method for hydrogen, we proceed by matching the period of the phase of the higher-order contributions in $\Psi(\vec{r},t)$ with the period of the phase induced by shifting $\psi_{\rm cl}(\vec{r},t)$ by a fraction of its period $T^*_{\rm cl}$. We then determine the coefficients in the expansion and the constraints on the times $t^*_{\rm frac}$. Finally, we show that the wave packet and the autocorrelation function are periodic with a period $T^*_{\rm frac}$ and we determine the allowed values of $T^*_{\rm frac}$.

Consider $\Psi(\vec{r},t)$ at the times $t^*_{\rm frac}$. An additional phase $\exp[2\pi i\theta^*_k]$ due to the higher-order corrections appears relative to the linear term, where

$$\theta^*_k=\frac{3\bar{n}^*p}{4q}k^2-\frac{m}{n}k^2-\frac{p}{q}k^3\ . \quad \text{(C1)}$$

As usual, terms of order $t^*_{\rm rev}/t^*_{\rm sr}\ll 1$ in the exponential have been neglected.

To simplify the analysis as much as possible, we choose the integers m and n so that θ^*_k reduces to the value of θ_k defined for hydrogen in Eq. (A3). This imposes

$$\frac{m}{n}=\frac{3p(\lambda\nu-\mu)}{4q\nu}\pmod 1\ , \quad \text{(C2)}$$

where the right-hand side is understood to be fully reduced. With this choice, the phase θ^*_k equals the phase θ_k for hydrogen given in Eq. (A3). It therefore has the same minimum period l under shifts in the summation index k as for hydrogen, given in Eq. (A4).

Note that if $\mu=0$, the definition (C2) for m/n reduces to the form in Eq. (A2) for hydrogen. The additional shift for $\mu\neq 0$ comes from the fractional part of $\bar{n}^*$ due to the quantum defect, assuming the laser is on resonance. We therefore see that the allowed times $t^*_{\rm frac}$ are *not* simply obtained by the scaling transformations $t_{\rm sr}\rightarrow t^*_{\rm sr}$ and $t_{\rm rev}\rightarrow t^*_{\rm rev}$ in the definition of $t_{\rm frac}$. In addition to the scaling, the fraction m/n is shifted by an amount that depends on the quantum defect.

We next consider the phase ϕ^*_k induced by shifting the classical waves $\psi_{\rm cl}(\vec{r},t)$ by an amount

$$\Delta t=\frac{a}{b}t^*_{\rm rev}+\frac{c}{d}T^*_{\rm cl}\ , \quad \text{(C3)}$$

where a,b and c,d are pairs of relatively prime integers. The phase generated is

$$\phi_k^* = \frac{2\bar{n}^* a}{3b} k + \frac{c}{d} k \ . \tag{C4}$$

Substituting the definition of $\bar{n}^*$ given in Eq. (28), we choose the integers c and d to satisfy

$$\frac{2(\lambda\nu-\mu)a}{3\nu b} + \frac{c}{d} = 0 \pmod 1 \ . \tag{C5}$$

With this condition, ϕ_k^* reduces to the expression (A8) for the phase ϕ_k in hydrogen.

Following the definitions in Eq. (A9), ϕ_k can be written as α/lk, where α and l are relatively prime integers as defined in Sec. III C. The time shifts Δt are then given by

$$\Delta t = \frac{\alpha}{l} T_{\rm cl}^* \ . \tag{C6}$$

The minimum period of ϕ_k^* under shifts in the summation index k is again l, which matches the period of θ_k^*.

Since the phases induced by the shifts Δt in $\psi_{\rm cl}(\vec{r},t)$ have the same period as the higher-order contributions to the time-dependent phase in $\Psi(\vec{r},t)$ at the times $t_{\rm frac}^*$, we may use the set $\psi_{\rm cl}(\vec{r},t_{\rm frac}^* + (s\alpha/l)T_{\rm cl}^*)$ with $s=0,1,\ldots,l-1$ as a basis for an expansion of $\Psi(\vec{r},t_{\rm frac}^*)$, and we obtain Eq. (30). Since the phases θ_k^* and ϕ_k^* have the same formal structure as those in hydrogen, the coefficients b_s may be taken to have the same form as in Eq. (14). The proof that this expansion is valid follows as before, using Eq. (A11).

The allowed values of q in the definition (27) of $t_{\rm frac}^*$ are restricted to multiples of 3. The proof follows that in hydrogen. Since the phase ϕ_k^* reduces to ϕ_k for hydrogen and since Eq. (A9) holds, the quantity $lN/3$ must again be an integer. This is true only if l and hence q are multiples of 3.

We next prove that the wave packet and absolute square of the autocorrelation function are periodic for times near $t_{\rm frac}^*$ and we determine the periodicity $T_{\rm frac}^*$. The procedure is similar to the corresponding proofs for hydrogen.

Consider the wave function $\Psi(\vec{r},t_{\rm frac}^*)$ under a shift in time $t_{\rm frac}^* \to t_{\rm frac}^* + (e/f)t_{\rm rev}^*$. It can be shown that the minimum shift that leads to periodic behavior is $e/f = 3/q$. The wave function at this shifted time can be written as an expansion in $\psi_{\rm cl}$ with coefficients b_s' given in Eq. (B5). In parallel with the hydrogenic case, for $p=1$ we find the relation $|b_s'| = |b_{(s+x)_{\rm mod}\, l}|$ for some integer x that can be shown to exist.

Taking the squared modulus of the wave function and using the assumption that the subsidiary waves do not overlap, we deduce

$$|\Psi(\vec{r},t_{\rm frac}^* + T_{\rm frac}^*)|^2 = |\Psi(\vec{r},t_{\rm frac}^*)|^2 \ , \tag{C7}$$

with the period $T_{\rm frac}^* = (3/q)t_{\rm rev}^* - (u/v)T_{\rm cl}^*$. The integers u and v satisfy a relation that depends on the fractional part of the quantum defect:

$$\frac{u}{v} = \frac{2(\eta+\lambda)-3}{q} - \frac{2\mu}{q\nu} \pmod 1 \ . \tag{C8}$$

Equation (C7) shows that near the times $t_{\rm frac}^*$ the wave packet is periodic with period $T_{\rm frac}^*$. Using a similar technique, we have proved that the square of the autocorrelation function is also periodic at the times $t_{\rm frac}^*$, with the same period $T_{\rm frac}^*$.

[1] J. Parker and C. R. Stroud, Phys. Rev. Lett. **56**, 716 (1986); Phys. Scr. **T12**, 70 (1986).

[2] G. Alber, H. Ritsch, and P. Zoller, Phys. Rev. A **34**, 1058 (1986); G. Alber and P. Zoller, Phys. Rep. **199**, 231 (1991).

[3] I. Sh. Averbukh and N. F. Perelman, Phys. Lett. A **139**, 449 (1989).

[4] M. Nauenberg, J. Phys. B **23**, L385 (1990).

[5] L. D. Noordam, D. I. Duncan, and T. F. Gallagher, Phys. Rev. A **45**, 4735 (1992).

[6] B. Broers, J. F. Christian, J. H. Hoogenraad, W. J. van der Zande, H. B. van Linden van den Heuvell, and L. D. Noordam, Phys. Rev. Lett. **71**, 344 (1993).

[7] J. F. Christian, B. Broers, J. H. Hoogenraad, W. J. van der Zande, and L. D. Noordam, Opt. Commun. **103**, 79 (1993).

[8] A. ten Wolde, L. D. Noordam, A. Lagendijk, and H. B. van Linden van den Heuvell, Phys. Rev. Lett. **61**, 2099 (1988).

[9] J. A. Yeazell, M. Mallalieu, J. Parker, and C. R. Stroud, Phys. Rev. A **40**, 5040 (1989).

[10] J. A. Yeazell, M. Mallalieu, and C. R. Stroud, Phys. Rev. Lett. **64**, 2007 (1990).

[11] J. A. Yeazell and C. R. Stroud, Phys. Rev. A **43**, 5153 (1991).

[12] D. R. Meacher, P. E. Meyler, I. G. Hughes, and P. Ewart, J. Phys. B **24**, L63 (1991).

[13] R. G. Hulet and D. Kleppner, Phys. Rev. Lett. **51**, 1430 (1983).

[14] D. Delande and J. C. Gay, Europhys. Lett. **5**, 303 (1988).

[15] Z. D. Gaeta, M. Noel, and C. R. Stroud, Phys. Rev. Lett. **73**, 636 (1994).

[16] See, for example, *Coherent States*, edited by J. R. Klauder and B.-S. Skagerstam (World Scientific, Singapore, 1985).

[17] R. Bluhm and V. A. Kostelecký, Phys. Rev. A **48**, R4047 (1993).

[18] R. Bluhm and V. A. Kostelecký, Phys. Rev. A **49**, 4628 (1994).

[19] L. S. Brown, Am. J. Phys. **41**, 525 (1973).

[20] J. Mostowski, Lett. Math. Phys. **2**, 1 (1977).

[21] M. M. Nieto, Phys. Rev. D **22**, 391 (1980); V. P. Gutschick and M. M. Nieto, *ibid.* **22**, 403 (1980).

[22] D. S. McAnally and A. J. Bracken, J. Phys. A **23**, 2027 (1990).

[23] M. Nauenberg, Phys. Rev. A **40**, 1133 (1989).

[24] J.-C. Gay, D. Delande, and A. Bommier, Phys. Rev. A **39**, 6587 (1989).

[25] Z. Dačić Gaeta and C. R. Stroud, Phys. Rev. A **42**, 6308 (1990).

[26] R. Bluhm and V. A. Kostelecký, Phys. Rev. A **50**, R4445 (1994).

[27] T. F. Gallagher, in *Rydberg States of Atoms and Molecules*, edited by R. F. Stebbings and F. B. Dunning (Cambridge University Press, Cambridge, 1983).

[28] R. Bluhm and V. A. Kostelecký, Phys. Lett. A **200**, 308 (1995).
[29] V. A. Kostelecký and M. M. Nieto, Phys. Rev. A **32**, 3243 (1985).
[30] V. A. Kostelecký, in *Symmetries in Science VII: Dynamic Symmetries and Spectrum-Generating Algebras in Physics,* edited by B. Gruber and T. Osaka (Plenum, New York, 1993).
[31] H. A. Bohr, *Almost Periodic Functions* (Chelsea, New York, 1947).
[32] A. Peres, Phys. Rev. A **47**, 5196 (1993).
[33] J. Wals, H. H. Fielding, J. F. Christian, L. C. Snoek, W. J. van der Zande, and H. B. van Linden van den Heuvell, Phys. Rev. Lett. **72**, 3783 (1994).
[34] T. F. Gallagher, *Rydberg Atoms* (Cambridge University Press, Cambridge, 1994).